



# **GEOLOGY FOR SOCIETY**

SINCE 1858



**GEOLOGICAL  
SURVEY OF  
NORWAY**

· NGU ·

**NGU REPORT**  
**2020.044**

---

Tomographic inversion of synthetic  
refraction seismic data.  
Quality of inversion using various off-  
end shots, fracture zone depth,  
fracture zone velocity, soil thickness  
and hidden layer thickness.





|   |  |   |   |                               |  |
|---|--|---|---|-------------------------------|--|
| <b>Report no.:</b> 2020.044   |  | <b>ISSN: 0800-3416 (print)</b><br><b>ISSN: 2387-3515 (online)</b> |   | <b>Grading:</b> Open          |  |
| <b>Title:</b><br>Tomographic inversion of synthetic refraction seismic data. Quality of inversion using various off-end shots, fracture zones depth, fracture zone velocity, soil thickness and hidden layer thickness.   |  |   |   |                               |  |
| <b>Authors:</b><br>Jan Steinar Rønning, Georgios Tassis,<br>Roger Wisén & Björn Toresson  |  |   | <b>Client:</b><br>Norwegian Public Roads Administration<br>(NPRA) / NGU |                               |  |
| <b>County:</b>  |  |   | <b>Commune:</b>   |                               |  |
| <b>Deposit name and grid-reference:</b>   |  |   | <b>Number of pages:</b> 57  |                               | <b>Price (NOK):</b> 150,-                          |
|   |  |   | <b>Map enclosures:</b>  |                               |  |
| <b>Fieldwork carried out:</b>   |  | <b>Date of report:</b><br>26.04.2021                              |   | <b>Project no.:</b><br>329500 | <b>Person responsible:</b><br><i>Marco Brønner</i> |
| <b>Summary:</b><br>NGU has studied tomographic inversion of refraction seismic data using the Rayfract software for years. In the present work, the quality of location and characterisation of fracture zones in bedrock as well as the quality of soil thickness calculation and characterisation is studied by modelling of synthetic data. The soil thickness is varied from a thin cover (1 – 5 m) to 20, 40 and 80 m. As a part of this work, the effect of distance to off-end shots outside the receiver spread are studied. Fracture zone velocity and depth extent are varied, and alternative inversion procedures are tested. Additional inversions were performed by Impakt Geofysik (Roger Wisén) using Geogiga DW Tomo.  |  |   |   |                               |  |
| Selected conclusions can be listed as follows:  |  |   |   |                               |  |
| <ul style="list-style-type: none"> <li>• The automatic Hagedoorn inversion of refraction seismic data gives a good image of fracture zones in bedrock under limited (&gt; 20 m) soil cover. A thicker soil cover presents challenges and demands traditional interpretation.</li> <li>• Due to poor resolution, thick fracture zones under a thick soil cover (&gt; 20 m) may consist of several thinner fractured zones.</li> <li>• The automatic Hagedoorn inversion of refraction seismic data gives a good image of the soil layers as long as the assumptions for using the method are fulfilled (increased velocity with depth, sub-horizontal homogenous layers, large velocity contrast).</li> <li>• An accuracy of 90 to 95 % of the average true soil thickness can be achieved with the Hagedoorn's method and following tomographic inversion. Hidden layers of increasing thickness may reduce the accuracy to ca. 80 % of true soil thickness. However, individual variations along the profiles may be larger.</li> <li>• Except in the case of hidden layers, the Hagedoorn inversion may give good velocity estimations that can be used for soil material characterisation.</li> <li>• The DeltatV and Geogiga inversion method shows a gradual increase of the velocity with depth, and a velocity isoline must be chosen as an indicator for bedrock surface. In the present work, we were able to find a velocity isoline that gave an average total thickness within +/- 8 % of the true soil thickness for the hidden layer models, which is very good. However, variations along the profiles varied from 78 % to 125 % of the real soil thickness.</li> <li>• The gradient velocity distribution in DeltatV inversion makes soil material characterisation challenging.</li> <li>• At least, one off-end shot should be more than three times the soil thickness away from both ends of the receiver spread.</li> <li>• A low RMS error do not guarantee for a correct velocity section.</li> <li>• Used in the right way, the Rayfract software can be used for the location and characterisation of fractured zones in bedrock as well as mapping and characterisation of soil layers. However, hidden layers (blind zones) seem to be a problem.</li> <li>• In this study we have tested just a few models, and during the work the Rayfract software is upgraded with new routines. More modelling is needed to get better understanding of how automatic inversion of refraction seismic data works, also with other available software.</li> </ul> |  |   |   |                               |  |
| <b>Keywords:</b>  |  | Geophysics  |   | Fracture zones                |  |
| Depth to bedrock  |  | Characterisation  |   | Refraction seismic            |  |
| Tomographic inversion   |  | Modelling   |   | Scientific report             |  |



## CONTENTS

|   |           |
|---|-----------|
| <b>1. INTRODUCTION .....</b>  | <b>7</b>  |
| <b>2. SOFTWARE AND INVERSION PROCEDURE DESCRIPTION.....</b>                           | <b>8</b>  |
| <b>3. MODELS AND SYNTHETIC DATA .....</b>   | <b>10</b> |
| <b>4. MODELING RESULTS.....</b>   | <b>13</b> |
| 4.1 Variations in remote shots at 20 m soil cover.....                                | 13        |
| 4.1.1 Fracture zone location and characterisation. ....                               | 14        |
| 4.1.2 Soil thickness and characterisation .....                                       | 15        |
| 4.2 Variations in off-end shots at 40 m soil cover.....                               | 17        |
| 4.2.1 Fracture zones location and characterisation.....                               | 17        |
| 4.2.2 Soil thickness and characterisation .....                                       | 17        |
| 4.3 Variations in off-end shots at 80 m soil cover.....                               | 20        |
| 4.3.1 Fracture zones location and characterisation.....                               | 20        |
| 4.3.2 Soil thickness and characterisation .....                                       | 20        |
| 4.4 Effect of varying fracture zone velocity and depth extent.....                    | 22        |
| 4.4.1 Varying fracture zone velocity and depth extent with thin soil cover .....      | 22        |
| 4.4.2 Varying fracture zone velocity and depth extent with 20 m soil cover.....       | 24        |
| 4.5 Effect of a blind zone above bedrock on depth estimations .....                   | 26        |
| 4.5.1 Effect of blind zone at a 40 m thick two-layered soil cover .....               | 26        |
| 4.5.2 Effect of blind zone at a 40 m thick three-layered soil cover .....             | 29        |
| 4.6 Alternative inversion of a two- and three-layered soil model.....                 | 31        |
| 4.6.1 NGU inversion using Rayfract and the DeltatV method .....                       | 31        |
| 4.6.2 IMPAKT inversion of Dataset G using software from Geogiga .....                 | 37        |
| 4.6.3 IMPAKT traditional interpretation of Dataset G1 .....                           | 39        |
| <b>5. DISCUSSION.....</b>   | <b>41</b> |
| 5.1 Detection and characterisation of fracture zones in bedrock .....                 | 41        |
| 5.1.1 Effect of increasing soil cover thickness using Hagedoorn's method .....        | 42        |
| 5.1.2 Detection and characterisation of fracture zones using the DeltatV method ..... | 43        |
| 5.1.3 Effect of fracture zone velocity and depth extent .....                         | 43        |
| 5.1.4 Fracture zone detection and characterisation with different methods .....       | 44        |
| 5.2 Depth to bedrock calculations .....   | 45        |
| 5.2.1 Quality of depth to bedrock calculations using Hagedoorn's method .....         | 45        |
| 5.2.2 Quality of depth to bedrock calculations using DeltatV method .....             | 48        |
| 5.2.3 Comparison of methods for depth to bedrock calculations .....                   | 49        |
| 5.3 Quality of soil material characterisation.....                                    | 51        |
| 5.3.1 Detection and characterisation of soil layers using Hagedoorn's method .....    | 51        |
| 5.3.2 Detection and characterisation of soil layers using DeltatV method. ....        | 52        |
| 5.3.3 Comparison of methods for soil material characterisation .....                  | 53        |
| 5.4 General considerations.....   | 53        |
| <b>6. CONCLUSIONS .....</b>   | <b>54</b> |
| <b>7. REFERENCES .....</b>  | <b>56</b> |



## 1. INTRODUCTION

The Geological Survey of Norway (NGU) has previously performed modelling using synthetic data from given models and the Rayfract<sup>®</sup> software (Tassis et al. 2017, Tassis et al. 2018). The modelling is performed by defining a physical model from which synthetic data are calculated. These synthetic data are inverted using different procedures, and by doing so, capabilities and limitations with the inversion procedures can be studied. From this work we have concluded that the assumed best procedure for mapping and characterisation of fracture zones in bedrock is to use the multi-run, Conjugate Gradient inversion method, with Cosine-Squared weighting and a starting model generated using the Hagedoorn plus-minus method. So far, NGU has only briefly studied the quality of depth to bedrock interpretation and soil characterisation.

In the first work, looking mostly at models with none or thin soil cover, we deemed it possible to locate and characterise fractured zones in bedrock, albeit with some limitations (Tassis et al. 2017). It was found that **imaging the position and inclination of zones** could be problematic, especially when the zones have small velocity contrast to the neighbouring bedrock. The detectable **depth extent** of fracture zones can be followed to a certain depth, but moderate deep zones gave the same response as deeper zones due to the limitations of the methods. The **width** of the zone is often quite close to reality, and **overburden layers** can be precisely defined when the interactive picking of branch points prior to inversion is carefully done. The **velocity** of a zone can be accurately calculated with a good combination of inversion parameters.

In the second work (Tassis et al. 2018), inversion using starting models generated with the DeltatV and the Wavefront methods (Intelligent resources 2019a and -b) were tested. The DeltatV method, which is based on diving waves, requires long lines (minimum 500 m) and dense receivers and shot coverage (receivers every 1 or 2 m and shots every 3<sup>rd</sup> of 4<sup>th</sup> receiver). A starting model generated by the DeltatV method and the dense receiver and shot-point spacing, did not improve the capability to locate and characterise fracture zones in bedrock compared with the results from Hagedoorn's plus-minus method generated starting models. However, a starting model generated by the Wavefront method can be a good alternative to Hagedoorn's method. From this work, we also could conclude that the semi-automatic picking of midpoint breaks is an alternative to time-consuming manual crossover point picking.

In this second work (Tassis et al. 2018), we also examined the effect of a low-velocity soil overburden could have on the success of tomographic inversion. A total soil thickness of 20 m and 40 m was tested using a 2 m receiver spacing and 6 m shot spacing. We concluded that for shorter lines, an overburden layer of 20 m could inhibit fracture zone detection but not entirely, while a 40 m of low-velocity top layer could critically limit resolution at depth. In this work, we had off-end shots at 30 and 60 m from the end of the receiver spreads. For the 40 m soil thickness, off-end shots further away may be necessary. This is tested in the present work as well as modelling of 80 m total soil thickness.

In subsea tunnel projects, two geologically related features are important; fracture zones in bedrock and soil thickness and type. Traditionally, this is solved by doing manually interpretation of refraction seismic data. The basic methods for calculating layers based on direct and refracted wave first breaks does not handle "velocity inversion" (decreasing velocity towards depth) and "hidden layer problem" (too thin layer to be detected, Reynolds 2011). However, an experienced interpreter can read a



lot out of data and either comment on uncertainty based on this or make assumptions that can be used to constrain the interpretation, so it may account for such features. It is interesting to see if tomographic inversion of refraction seismic data can overcome these problems.

Westerdal (2003) showed that a 10 m deep depression in the bedrock topography could be misinterpreted as a fracture zone in bedrock with extremely bad bedrock quality using Hagedoorn's method. To see if tomographic inversion can overcome this problem, we have modelled a fracture zone with varying depth extent. We have also varied the velocity in the fracture zones with or without soil cover.

In the present work, the ability to map soil thickness is investigated. For this work, the DeltatV method of generating a starting model was also tested.

Georgios Tassis conducted the modelling using Rayfract. Jan S. Rønning designed the modelling program and prepared the report. Roger Wisén has performed inversion of one dataset using the software DW Tomo from the company Geogiga (2019). Björn Toresson did the traditional interpretation of one line. Many thanks to Anne Liinamaa-Dehls who improved the English language.

## **2. SOFTWARE AND INVERSION PROCEDURE DESCRIPTION**

The Rayfract<sup>®</sup> software can process both p- and s-wave refraction seismic (Intelligent Resources 2019a and 2018b). The software can create velocity profiles automatically and is assumed to better handle velocity variations within layers, thinning of layers, faults and other velocity anomalies (Intelligent Resources 2019a). We are interested in seeing how the tomographic inversion can handle classical velocity inversions and blind zones.

The processing flow can be divided into three steps: File preparation, Initial model creation and WET (Wavepath Eikonal Traveltime) inversion. A flowchart is presented in Figure 1. The first step is to organize the data and data files.

The second step is to produce a starting model for the final tomographic inversion. A starting model can be created in five different ways (see Figure 1):

1. Import a custom made 2D starting model (Intelligent Resources 2019a)
2. Create a 2D starting model using the Wavefront method (Bruckl 1987, Ak 1990)
3. Create a 2D starting model using Hagedoorn's +/- method (Hagedoorn 1959)
4. Create a 2D starting model using the DeltatV method (Gebrande & Miller 1985)
5. Create a 1D Gradient starting model (Intelligent Resources 2019a).

NGU has tested most of the above (not no. 1) for fracture zone characterisation and found that using the Hagedoorn plus-minus-method is suitable not only to create a starting model for the inversion but can also act as an independent interpretation. In principle, this is the same method used traditionally for fracture zone detection/characterisation and soil thickness mapping/characterisation.

The inversion can be executed simply as an "Automatic (smooth) Inversion". However, the more advanced inversion routines shown to the left in Figure 1 have proven to be better. NGU has experienced that the best procedure to map fracture zones in bedrock

is to create a starting model with Hagedoorn’s plus-minus-method, then do a multi-run Conjugate Gradient inversion, use a Cosine-Squared weighting and minimal smoothing (Tassis et al. 2017 and 2018, Rønning et al. 2019a and -b). In the modelling presented in this report, we have followed our standard procedure in most cases. For each run in the Multi-run mode, we decrease the wavepath width in steps of 2 % from 30 % to 12 %, which means 9 individual inversion runs.

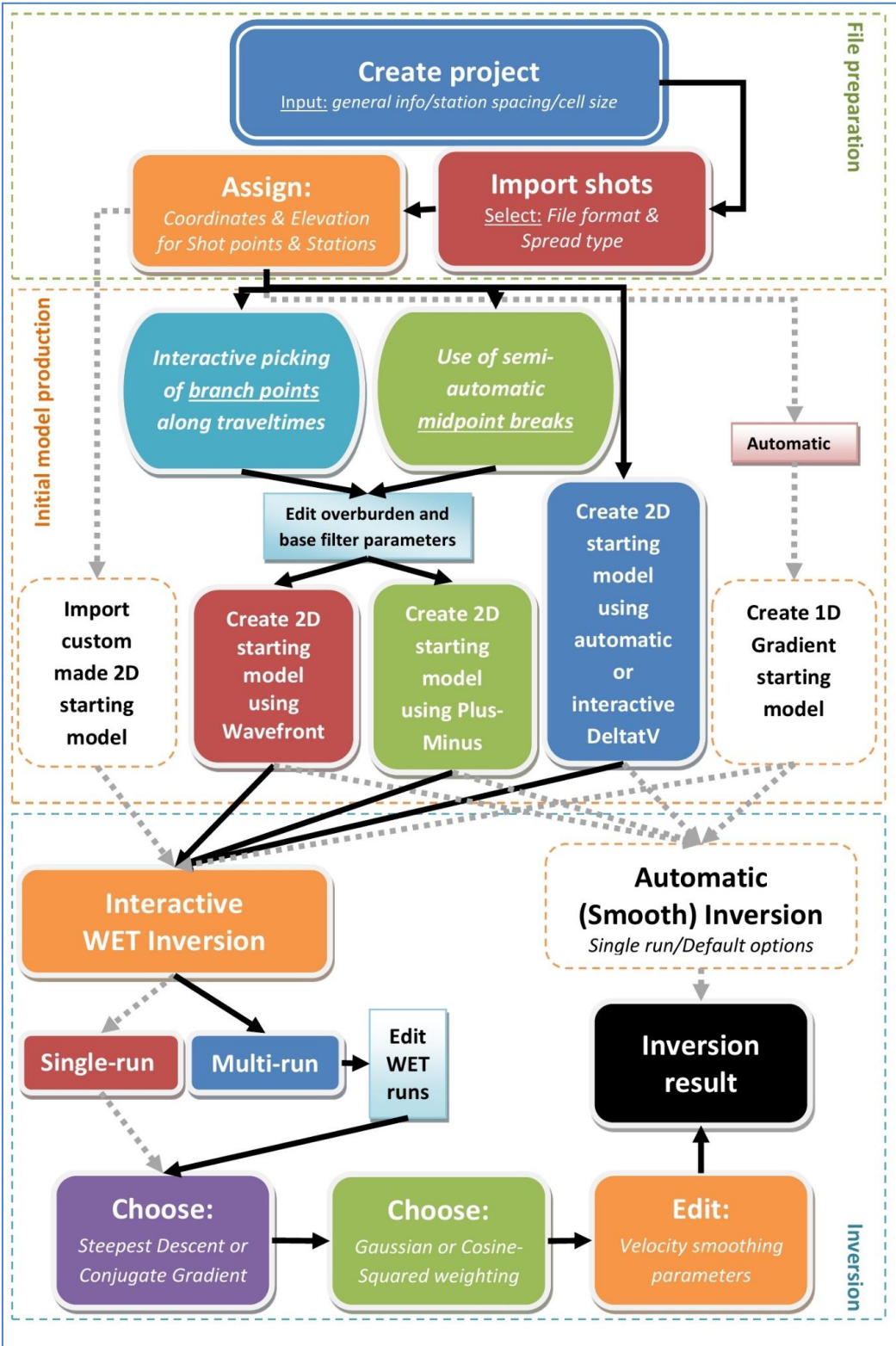


Figure 1: Flowchart for Rayfract® software. Black arrows show procedures we have used in the modelling work and grey dotted arrows other options available with the software.

To study the preferred procedure for soil thickness mapping, we used the DeltatV method for generating a starting model. The tomographic inversion followed the same procedure as with the Hagedoorn generated starting model.

### 3. MODELS AND SYNTHETIC DATA

The basis for the modelling effort presented in this report, is borrowed from the traditional Hagedoorn Plus-Minus interpretations performed for profiles P1-1 from Knappe tunnel in Bergen (Wåle 2009). The model is shown in **Figure 2**. P1-1 presents three subsequent fracture zones (velocity 3800 m/s and width 15, 10 and 10 m respectively) with thin overburden (1 – 5 m). The base models were constructed as a grid in Surfer 15 (Golden Software 2018) and then imported into Rayfract® for traveltimes calculation according to specified shot and receiver spacings (forward modelling, Intelligent Resources 2019b). Synthetic data based on this model were also constructed in the past (Tassis et al. 2017 and 2018). In the present work we focus on distance to off-end shots, using shot and geophone spacing of 20 m and 5 m respectively which is commonly used in Norway. All the varying details about the modelling are presented in Table 1A and Table 1B.

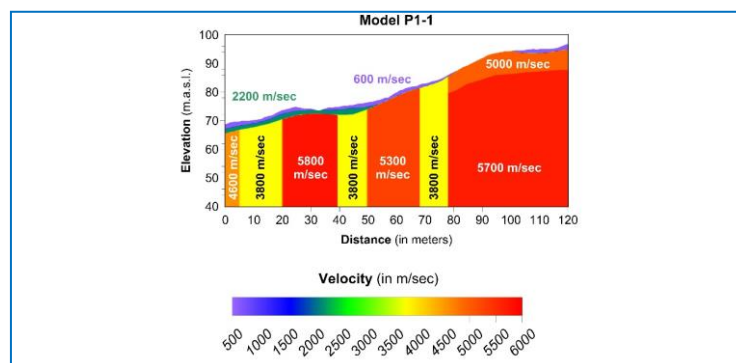


Figure 2: Surfer 15 grids based on traditional interpretations done for profile P1-1 from Knappe tunnel (Wåle 2009). Elevation in meters above sea level (m.a.s.l.).

In the present modelling, the synthetic model shown in Figure 2 was used as a basic model. In the first three sets of modelling (Table 1A), we tested the effect of varying the distance to the off-end shots where the total soil thickness varies from 20 m (Dataset A), 40 m (Dataset B) and 80 m (Dataset C). The soil cover consists of a 5 m thick layer with a velocity of 600 m/s on top of a layer with a velocity of 1600 m/s that has a thickness of 15 m, 35 m and 75 m respectively. This is a complex model that challenge the software’s ability to identify and characterise fracture zones in bedrock as well as mapping and characterisation of the soil.

In the fourth set of modelling (Dataset D), we varied the velocity in the fracture zones and the depth extent of the second fracture zone from 5 m to 10 m and 20 m in addition to a full depth. A full depth means a depth deeper than the penetration depth of the seismic rays. Here, the soil cover was simulated to be from 0 to 5 m, as shown on the original data from the Knappe tunnel in Bergen (Wåle 2009). In this way, we expect to see if false interpreted fracture zones, because of bedrock depressions (Westerdahl 2003), can be processed away by the tomographic inversion. In the fifth set of modelling (Dataset E), we did the same as in Dataset D, but the total soil thickness is 20 m.

Table 1A: Synthetic models used to study effects of variation in off-end shot distance (dataset A, B and C), fracture zone depth and fracture zone velocity (dataset D and E). Interpreted depth to bedrock and fracture zone location and geometry are discussed in the text. Deviation from standard model marked in pink.

| Model | Soil thickness<br>Layer 1 +<br>Layer 2 (m) | Velocity<br>Zone 1<br>(m/s) | Velocity<br>Zone 2<br>(m/s) | Velocity<br>Zone 3<br>(m/s) | Velocity<br>Zone 4<br>(m/s) | Velocity<br>Background<br>(m/s) | Depth<br>Zone 1<br>(m) | Depth<br>Zone 2<br>(m) | Depth<br>Zone 3<br>(m) | Depth<br>Zone 4<br>(m) | Distance shot (m)        |
|-------|--|-----------------------------|-----------------------------|-----------------------------|-----------------------------|---------------------------------|------------------------|------------------------|------------------------|------------------------|--------------------------|
| A1    | 5 + 15 = 20                                | 4600                        | 3800                        | 3800                        | 3800                        | 5500                            | Full                   | Full                   | Full                   | Full                   | 30                       |
| A2    | 5 + 15 = 20                                | 4600                        | 3800                        | 3800                        | 3800                        | 5500                            | Full                   | Full                   | Full                   | Full                   | 30 + 60                  |
| A3    | 5 + 15 = 20                                | 4600                        | 3800                        | 3800                        | 3800                        | 5500                            | Full                   | Full                   | Full                   | Full                   | 30 + 60 + 90             |
| B1    | 5 + 35 = 40                                | 4600                        | 3800                        | 3800                        | 3800                        | 5500                            | Full                   | Full                   | Full                   | Full                   | 30                       |
| B2    | 5 + 35 = 40                                | 4600                        | 3800                        | 3800                        | 3800                        | 5500                            | Full                   | Full                   | Full                   | Full                   | 30 + 60                  |
| B3    | 5 + 35 = 40                                | 4600                        | 3800                        | 3800                        | 3800                        | 5500                            | Full                   | Full                   | Full                   | Full                   | 30 + 60 + 90             |
| B4    | 5 + 35 = 40                                | 4600                        | 3800                        | 3800                        | 3800                        | 5500                            | Full                   | Full                   | Full                   | Full                   | 30 + 60 + 90 + 120       |
| B5    | 5 + 35 = 40                                | 4600                        | 3800                        | 3800                        | 3800                        | 5500                            | Full                   | Full                   | Full                   | Full                   | 30 + 60 + 90 + 120 + 150 |
| C1    | 5 + 75 = 80                                | 4600                        | 3800                        | 3800                        | 3800                        | 5500                            | Full                   | Full                   | Full                   | Full                   | 60                       |
| C2    | 5 + 75 = 80                                | 4600                        | 3800                        | 3800                        | 3800                        | 5500                            | Full                   | Full                   | Full                   | Full                   | 60 + 120                 |
| C3    | 5 + 75 = 80                                | 4600                        | 3800                        | 3800                        | 3800                        | 5500                            | Full                   | Full                   | Full                   | Full                   | 60 + 120 + 180           |
| C4    | 5 + 75 = 80                                | 4600                        | 3800                        | 3800                        | 3800                        | 5500                            | Full                   | Full                   | Full                   | Full                   | 60 + 120 + 180 + 240     |
| D1    | 0 - 3                                      | 4600                        | 3800                        | 2800                        | 2800                        | 5500                            | Full                   | Full                   | Full                   | Full                   | 30 + 60                  |
| D2    | 0 - 3                                      | 4600                        | 3800                        | 2800                        | 2800                        | 5500                            | Full                   | Full                   | 5                      | Full                   | 30 + 60                  |
| D3    | 0 - 3                                      | 4600                        | 3800                        | 2800                        | 2800                        | 5500                            | Full                   | Full                   | 10                     | Full                   | 30 + 60                  |
| D4    | 0 - 3                                      | 4600                        | 3800                        | 2800                        | 2800                        | 5500                            | Full                   | Full                   | 20                     | Full                   | 30 + 60                  |
| E1    | 5 + 15 = 20                                | 4600                        | 2800                        | 3800                        | 4800                        | 5500                            | Full                   | Full                   | Full                   | Full                   | 30 + 60 + 90             |
| E2    | 5 + 15 = 20                                | 4600                        | 2800                        | 3800                        | 4800                        | 5500                            | Full                   | Full                   | 5                      | Full                   | 30 + 60 + 90             |
| E3    | 5 + 15 = 20                                | 4600                        | 2800                        | 3800                        | 4800                        | 5500                            | Full                   | Full                   | 10                     | Full                   | 30 + 60 + 90             |
| E4    | 5 + 15 = 20                                | 4600                        | 2800                        | 3800                        | 4800                        | 5500                            | Full                   | Full                   | 20                     | Full                   | 30 + 60 + 90             |

Table 1B: Synthetic models used to study the effects of variation of hidden layer thickness. In dataset F, the hidden layer,  $V = 2100$  m/s in a soil environment of 1600 m/s, is 0, 5, 10 and 20 m thick. Dataset G is the same as dataset F with a 5 m thick surface layer with a velocity 600 m/s (dry soil). Deviation from standard model marked in pink.

| Model | Soil thickness<br>Layer 1 + Layer 2 +<br>Layer 3 (m) | Velocity<br>Zone 1<br>(m/s) | Velocity<br>Zone 2<br>(m/s) | Velocity<br>Zone 3<br>(m/s) | Velocity<br>Zone 4<br>(m/s) | Velocity<br>Background<br>(m/s) | Depth<br>Zone 1<br>(m) | Depth<br>Zone 2<br>(m) | Depth<br>Zone 3<br>(m) | Depth<br>Zone 4<br>(m) | Distance shot (m)  |
|-------|--|-----------------------------|-----------------------------|-----------------------------|-----------------------------|---------------------------------|------------------------|------------------------|------------------------|------------------------|--------------------|
| F1    | 0 + 40 + 0 = 40                                      | 4600                        | 3800                        | 3800                        | 3800                        | 5500                            | Full                   | Full                   | Full                   | Full                   | 30 + 60 + 90 + 120 |
| F2    | 0 + 35 + 5 = 40                                      | 4600                        | 3800                        | 3800                        | 3800                        | 5500                            | Full                   | Full                   | Full                   | Full                   | 30 + 60 + 90 + 120 |
| F3    | 0 + 30 + 10 = 40                                     | 4600                        | 3800                        | 3800                        | 3800                        | 5500                            | Full                   | Full                   | Full                   | Full                   | 30 + 60 + 90 + 120 |
| F4    | 0 + 20 + 20 = 40                                     | 4600                        | 3800                        | 3800                        | 3800                        | 5500                            | Full                   | Full                   | Full                   | Full                   | 30 + 60 + 90 + 120 |
| G1    | 5 + 35 + 0 = 40                                      | 4600                        | 3800                        | 3800                        | 3800                        | 5500                            | Full                   | Full                   | Full                   | Full                   | 30 + 60 + 90 + 120 |
| G2    | 5 + 30 + 5 = 40                                      | 4600                        | 3800                        | 3800                        | 3800                        | 5500                            | Full                   | Full                   | Full                   | Full                   | 30 + 60 + 90 + 120 |
| G3    | 5 + 25 + 10 = 40                                     | 4600                        | 3800                        | 3800                        | 3800                        | 5500                            | Full                   | Full                   | Full                   | Full                   | 30 + 60 + 90 + 120 |
| G4    | 5 + 15 + 20 = 40                                     | 4600                        | 3800                        | 3800                        | 3800                        | 5500                            | Full                   | Full                   | Full                   | Full                   | 30 + 60 + 90 + 120 |

In the sixth set of modelling (Dataset F, Table 1B), we tried to see if a “hidden layer” (Reynolds 2011) could be detected or indicated by tomographic inversion. In this case, the total soil thickness was 40 m. By traditional and automatic (Rayfract) interpretation using Hagedoorn’s plus-minus-method, it can be physically impossible to see a thin layer despite having increased velocity towards the depth. Dataset G is almost the same as Dataset F, but with a 5 m thick dry soil layer on the top (600 m/s).

The Hagedoorn method is not able to see a “hidden layer” (Reynolds 2011). The starting model is often inherited in the inversion process. To see if an unbiased method can give better soil thickness estimations than with the Hagedoorn starting model, dataset F and G was inverted using a starting model generated by the DeltatV method (Figure 1). Roger Wisén at Impakt Geofysik AB inverted the dataset F using software from Geogiga (2019).

## **4. MODELING RESULTS**

In this chapter, the modelling results are presented. The basic synthetic fracture models are presented in Figure 2 and Table 1A and 1B. Common for all models are a receiver spacing 5 m and a shotpoint spacing 20 m inside the receiver spread. In most of the modelling, the starting models are created using Hagedoorn’s plus-minus-method and semi-automatic picking of midpoint breaks (see Figure 1 and Intelligent Resources 2019a). In two cases (dataset F and G), the starting model was generated also by using the DeltatV method. The inversions are performed using the multi-run Conjugate Gradient method, Squared Weighting and minimal smoothing, a procedure which we previously have found to be the “assumed best procedure” for fracture (Tassis et al. 2017 and 2018). In addition, IMPAKT Geofysik has inverted Dataset G.

Most of the figures are presented in the same order: The synthetic model on the top, then the starting model created with Hagedoorn’s plus-minus-method or DeltatV method which also may be a valid interpretation, then the WET inversion and finally at the bottom the ray coverage.

In our soil thickness summary tables, we mark the average deviation from true thickness less than 2 % in deep green, deviation 2 % – 10 % in light green, 10 % to 20 % in yellow and deviations greater than 20 % in red (see also Rønning et al. 2020). Traditionally, the accuracy demand in refraction seismic is +/- 10 % of the true depth (Sjøgren 1984).

### **4.1 Variations in remote shots at 20 m soil cover**

The results of the modelling of dataset A with 20 m soil cover (5 m of velocity 600 m/s above 15 m with velocity 1600 m/s) are shown in Figure 3. In this section, we describe the images, noting the fracture zones location/characterisation and the soil thickness/characterisation.

#### 4.1.1 Fracture zone location and characterisation.

Previous work using the synthetic model presented in Figure 2 (soil thickness 1 – 5 m) with receiver spacing 5 m and shot-point spacing 30 m, 20 m and 15 m showed good inversion images both for the Hagedoorn plus-minus-method and the tomographic inversions using the “assumed best procedure” (Figure 6.2.1, Tassis et al. 2017). In a later work (Tassis et al. 2018), a new test where the total soil thickness was 20 m and 40 m and the receiver spacing 2 m and shotpoint spacing 6 and 8 m were performed. Hagedoorn’s method indicated all three fracture zones under the 20 m soil cover, and with a good velocity and thickness fit. However, the first of the zones was shifted ca. 5 m to the left (Figure 7.1.1, Tassis et al. 2018). Under a total soil cover of 40 m, both Hagedoorn’s method and the tomographic inversion failed to locate one of the fracture zones, and the two others were shifted ca. 10 m to the right (Figure 7.1.1, Tassis et al. 2018). This indicated that automatic locating and characterising fracture zones in bedrock under thick soil cover can be challenging.

At traditional refraction seismic surveys in Norway, the most common receiver spacing is 5 m and shot spacing 30 m to 50 m both for land and subsea surveys. In some surveys, the total soil cover can be as much as 100 m or more. Because of this, it was interesting to see how thick soil cover and different off-end shots will influence the likelihood of locating and characterising fracture zones in bedrock.

In Figure 3 we show the modelled data for dataset A1 (off-end shots at 30 m), A2 (off-end shots at 30 m and 60 m) and A3 (off-end shots at 30 m, 60 m and 90 m), all three with total soil cover of 20 m. Receiver spacing is 5 m and in spread shot spacing is 15 m – 20 m.

Dataset A1 indicate only two of the three fracture zones in the synthetic model at the **Hagedoorn** interpretation. The zones are slightly shifted sideways, the velocity is partly not correct, and the zone thickness do not fit. However, the velocities in solid bedrock fits at the end part of the profile. At the start of the profile, it seems impossible to resolve the low-velocity zone (4600 m/s) and the first fractured zone with velocity 3800 m/s, and they show up as a homogeneous section with velocity slightly above 4500 m/s.

In dataset A2 and A3 with more off-end shots, the **Hagedoorn** method improves the image of the fracture zones. The two datasets give a good image of zone 2 and 3, the thickness and velocity fit well, but the zones are shifted sideways by ca. 5 m. The 4600 m/s zone and the first 3800 m/s zone merge into one zone with velocity ca. 3500 m/s at the profile start.

The **tomographic inverted** images show almost the same fractures as the Hagedoorn interpretation but are more diffuse. Increased off-end shot number improves the images but this is most likely caused by a better Hagedoorn interpretation since the tomographic WET inversion do not use data from off-end shots (Intelligent Resources 2019a). The ray cover does not give a significant deeper penetration with increasing numbers of shots due to the same reason.

#### 4.1.2 Soil thickness and characterisation

Hagedoorn's **plus-minus-method** interpretation for dataset A1 (20 m soil cover, off-end shots at 30 m from the end receivers) gives a relatively good image of the soil cover (Figure 3). On top, we see a ca. 5 m thick layer with ca. velocity 600 m/s as in the starting model for all three off-end shot variations. Underneath this layer, the second soil layer appears with a velocity of ca. 1600 m/s. However, the total thickness is a bit less than in the synthetic mode (Table 2). In the beginning of the profile, the total soil thickness is ca. 19 m (95 % of true thickness). From ca. position 40 m, the total soil thickness is ca. 16,5 m which is 83 % of the true thickness. At the end of the profile, the thickness is almost 18 m (90 % of true thickness).

The **tomographic inversion** of the same profile shows a good image of the soil layers. However, the soil velocities seem to vary a bit around 600 m/s in layer 1 and around 1600 m/s in layer 2. The total soil thickness seems to fit the true values.

To get a quantitative image of the interpreted soil thickness variations, depths at the start, at the end and under each shot along the profile, are shown as an interval in Table 2, both in meters and in percent of the true depth. To get a number for the total deviation, the average of the 8 – 9 depth readings along the profile is calculated including standard deviations. For dataset A1 the average soil thickness is  $17.9 \pm 0.9$  m which is 89.4 % of the true depth for Hagedoorn's interpretation. For the tomographic inversion using Hagedoorn interpretation as a starting model (Table 2), these numbers are  $18.2 \pm 0.8$  m and 90.8 % of the true depth.

The same analysis as for Dataset A1 is performed for Dataset A2 and A3. The results are summarized in Table 2 both for the Hagedoorn starting model interpretation and for the tomographic inversion using Hagedoorn interpretation as a starting model.

Table 2: Inverted soil velocities and thickness in meters and in percent of true thickness from dataset A, 20 m soil thickness. Mean soil thickness is given in percent of the true soil thickness.

| Dataset, true soil thickness | Inversion method | Velocity V1 (m/s) | Velocity V2 (m/s) | Total soil thickness variation (m) | Total soil thickness variation in % | Mean soil thickness $\pm$ SDEV (m) | Mean soil thickness in % of true thickness |
|------------------------------|------------------|-------------------|-------------------|------------------------------------|-------------------------------------|------------------------------------|--|
| A1, 20 m                     | Hagedoorn        | $\approx 600$     | $\approx 1600$    | 16.5 - 19.0                        | 83 - 95                             | $17.9 \pm 0.9$                     | $89.4 \pm 4.0$                             |
| A1, 20 m                     | Tomography       | $\approx 600$     | 1500-2000         | 17.0 – 19.0                        | 85 - 95                             | $18.2 \pm 0.8$                     | $90.8 \pm 4.0$                             |
| A2, 20 m                     | Hagedoorn        | $\approx 600$     | $\approx 1600$    | 16.5 - 20.0                        | 83 - 100                            | $18.4 \pm 1.0$                     | $92.2 \pm 4.6$                             |
| A2, 20 m                     | Tomography       | $\approx 600$     | 1500-2000         | 17.0 - 20.0                        | 85 - 100                            | $19.0 \pm 1.0$                     | $95.0 \pm 5.0$                             |
| A3, 20 m                     | Hagedoorn        | $\approx 600$     | $\approx 1600$    | 16.0 - 20.0                        | 80 - 100                            | $18.5 \pm 1.6$                     | $92.5 \pm 7.4$                             |
| A3, 20 m                     | Tomography       | $\approx 600$     | 1500-2000         | 16.0 - 19.0                        | 80 - 95                             | $18,4 \pm 1.4$                     | $92.5 \pm 7.0$                             |

Hagedoorn's method gives very good soil velocity calculations. At the tomographic inversion, the soil velocity varies a bit more, but still provides good values. The total soil thickness varies from 16 m to 20 m and is always less or equal to the true soil thickness. On average, the total soil thickness varies from ca. 90 % to 95 % of the true soil thickness. Tomographic inversion improves the fit of the total soil thickness by about 2 – 3 % except for Dataset A3. More remote shots (Datasets A2 and A3) improve the total soil thickness interpretation by less than 2 %.



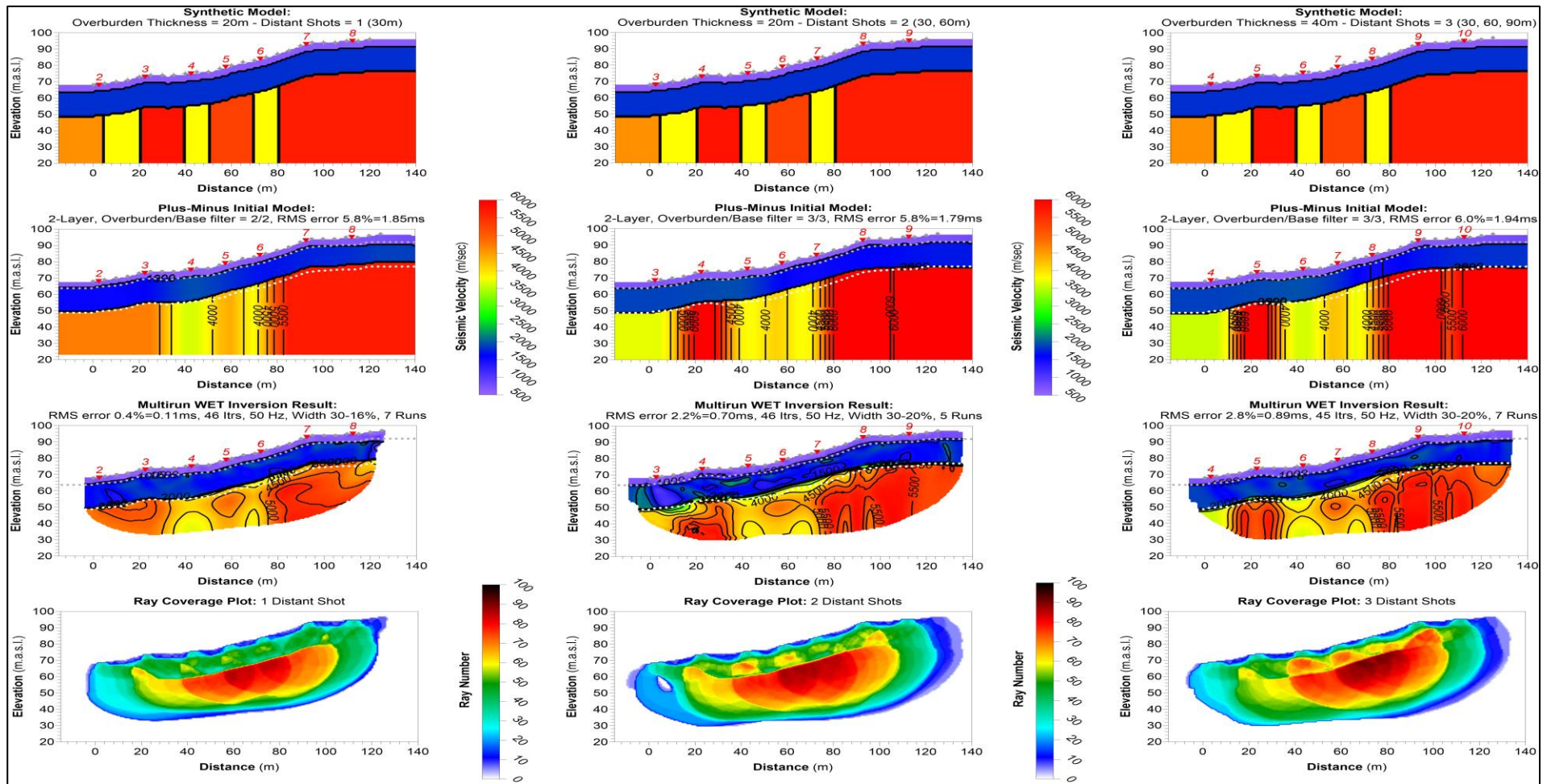


Figure 3: Modeling of the effect of off-end shots where the total soil thickness is 20 m. To the left: Dataset A1, off-end shot at 30 m from the spread. Middle: Dataset A2, off-end shots at 30 m and 60 m from the spread. To the right: Dataset A3, off-end shots at 30 m, 60 m and 90 m from the receiver spread. True layer interfaces are marked as a white dotted line.

## 4.2 Variations in off-end shots at 40 m soil cover

The results of the modelling with 40 m soil cover are shown in Figure 4. In the following section, we describe the images noting the fracture zones location/characterisation and the soil thickness/characterisation.

### 4.2.1 Fracture zones location and characterisation

In Datasets B1 and B2 (off-end shots 30 m and 30 + 60 m from receiver spread) , it is not possible to look through the 40 m thick soil and gives no information on fracture zone location and characterisation, neither at the Hagedoorn interpretation nor at the tomographic inversion.

Datasets B3, B4 and B5 allow us to view through the 40 m thick soil cover but cannot resolve the three fracture zones. At **Hagedoorn's interpretation** of Dataset B3, the three fracture zones with velocity 3800 m/s and the low-velocity zone (4600 m/s) at the beginning of the profile, merges into a 30 m wide zone with a velocity above 4000 m/s (position 0 – 30 m) followed by a ca. 30 m wide zone with ca. velocity 3500 m/s (position 30 – 60 m). At Dataset B4 and B5, using more off-end shots, the first of these shows higher velocity (> 4500 m/s) as in the synthetic model. The second fracture zone from position 30 – 60 m gets a sharper image and a lower velocity in the interval 3500 – 4000 m/s, not far from the initial fracture zone velocity.

The **tomographic inversion** shows a similar image of the fracture zones as with the Hagedoorn method, but a bit more diffuse. More off-end shots improve the visual image, but this does not allow for a better resolution of the fracture zones.

The ray coverage at the bottom of Figure 4 demonstrates how a greater length to off-end shots can improve the penetration depth. However, this is an effect of the penetration with the Hagedoorn interpretation since off-end shots are not accounted for in the tomographic inversion. The number of rays at the deepest parts is insufficient to give a good resolution of the fracture zones. The lack of data in the lower right part of Dataset B3 is an error in the plot that does not influence the tomographic inversion.

Location and characterisation of fracture zones under a 40 m thick soil cover using the Rayfract Hagedoorn method is challenging with a 5 m receiver spacing and a 20 m shot point spacing and the assumed best inversion procedure we have used.

### 4.2.2 Soil thickness and characterisation

The starting model for Dataset B1 and B2 (40 m total soil cover, off-end shots at 30 m and 30 m + 60 m from end receivers) created with **Hagedoorn's plus-minus-method**, do not reach down to bedrock. Ray coverage is limited to ca. 20 – 30 m below surface. The off-end shots are too close to the receiver spread to be able to interpret the total soil thickness. For the Datasets B3, B4, and B5, it is possible to see the soil/bedrock interface, but the total soil thickness is a bit too low. All five datasets seem to provide a good image of the first layer thickness and velocity. The total soil

thickness from interpreted images is compared with the total soil thickness in the synthetic model, and the results are summarized in Table 3. Also here, depth to bedrock is estimated at the start and the end of the profile and under each shotpoint.

The **tomographic inversion** of the same profile also shows a good image of the first soil layer with a velocity close to the true 600 m/s and thickness of ca. 5 m. As with Hagedoorn's interpretation, the tomographic inversion fails to map the thickness of soil layer 2 in Datasets B1 and B2, and the velocity of the layer varies in a horizontal gradient from ca. 1000 m/s to ca. 2500 m/s. In Dataset B3 (off-end shots at 30 m, 60 m and 90 m), the tomographic inverted image shows a confusing velocity variation in soil layer 2, which is believed to be an artificial effect. The soil/bedrock interface falls within a velocity gradient and it seems like this interface lies more or less at the 3000 m/s isoline. More off-end shots (Dataset B4 and B5) seem to compress this gradient. In the interpretation of the total soil thickness shown in Table 3, we use a velocity contour 3000 m/s as an indicator of the soil-bedrock interface.

Table 3: Inverted soil velocities and thicknesses in metres and percent of true thickness from Dataset B, 40 m soil thickness. Mean soil thickness is given in percent of the true soil thickness.

| Dataset, True soil thickness | Inversion method | Velocity V1 (m/s) | Velocity V2 (m/s) | Total soil thickness variation (m) | Total soil thickness variation in (%) | Mean soil thickness $\pm$ SDEV (m) | Mean soil thickness in % of true thickness |
|------------------------------|------------------|-------------------|-------------------|------------------------------------|---------------------------------------|------------------------------------|--|
| B1, 40 m                     | Hagedoorn        | $\approx$ 600     | 1500-2500         | ?                                  | ?                                     | ?                                  | ?  |
| B1, 40 m                     | Tomography       | $\approx$ 600     | 1500-2500         | ?                                  | ?                                     | ?                                  | ?  |
| B2, 40 m                     | Hagedoorn        | $\approx$ 600     | 1500-2500         | ?                                  | ?                                     | ?                                  | ?  |
| B2, 40 m                     | Tomography       | < 1000            | 1500-2500         | ?                                  | ?                                     | ?                                  | ?  |
| B3, 40 m                     | Hagedoorn        | $\approx$ 600     | $\approx$ 1600    | 34 - 40                            | 85 - 100                              | 37.4 $\pm$ 1.9                     | 93.6 $\pm$ 4.9                             |
| B3, 40 m                     | Tomography       | < 1000            | 1500-2000         | 35 - 45                            | 88 - 113                              | 38.7 $\pm$ 3.5                     | 96.7 $\pm$ 8.8                             |
| B4, 40 m                     | Hagedoorn        | $\approx$ 600     | $\approx$ 1600    | 36 - 40                            | 90 - 100                              | 37.9 $\pm$ 1.5                     | 94.7 $\pm$ 3.6                             |
| B4, 40 m                     | Tomography       | < 1000            | 1500-2000         | 34 - 42                            | 85 - 105                              | 38.0 $\pm$ 2.5                     | 95.0 $\pm$ 6.3                             |
| B5, 40 m                     | Hagedoorn        | $\approx$ 600     | $\approx$ 1600    | 34 - 40                            | 85 - 100                              | 37.7 $\pm$ 2.2                     | 94.2 $\pm$ 5.6                             |
| B5, 40 m                     | Tomography       | < 1000            | 1500-2000         | 34 - 40                            | 85 - 100                              | 37.0 $\pm$ 2.2                     | 92.5 $\pm$ 5.5                             |

From the data shown in Table 3, we can conclude that for a 40 m total soil cover, we need to place off-end shots at least 120 m away from the receiver spread on both ends. This fits well with the traditional rule of thumb: "off-end shots should be at least three times the soil thickness from the receiver spread". **Hagedoorn's plus-minus** method shows a good estimate of soil velocity and the total soil thickness is in average ca. 93 % of the true soil thickness. However, the soil thickness can vary from 34 m to the true thickness 40 m giving a standard deviation of about 2 %. **Tomographic inversion** using the Hagedoorn inverted model as a starting model, results partly in less accurate soil velocities as shown in Figure 4 and Table 3. Soil thickness estimates, using the velocity contour 3000 m/s as an indicator, varies in average from 96.7 % of the true thickness (Dataset B3) to 92.5 % for Dataset B5. Surprisingly, the average soil thickness decreases as the number of off-end shots increases.

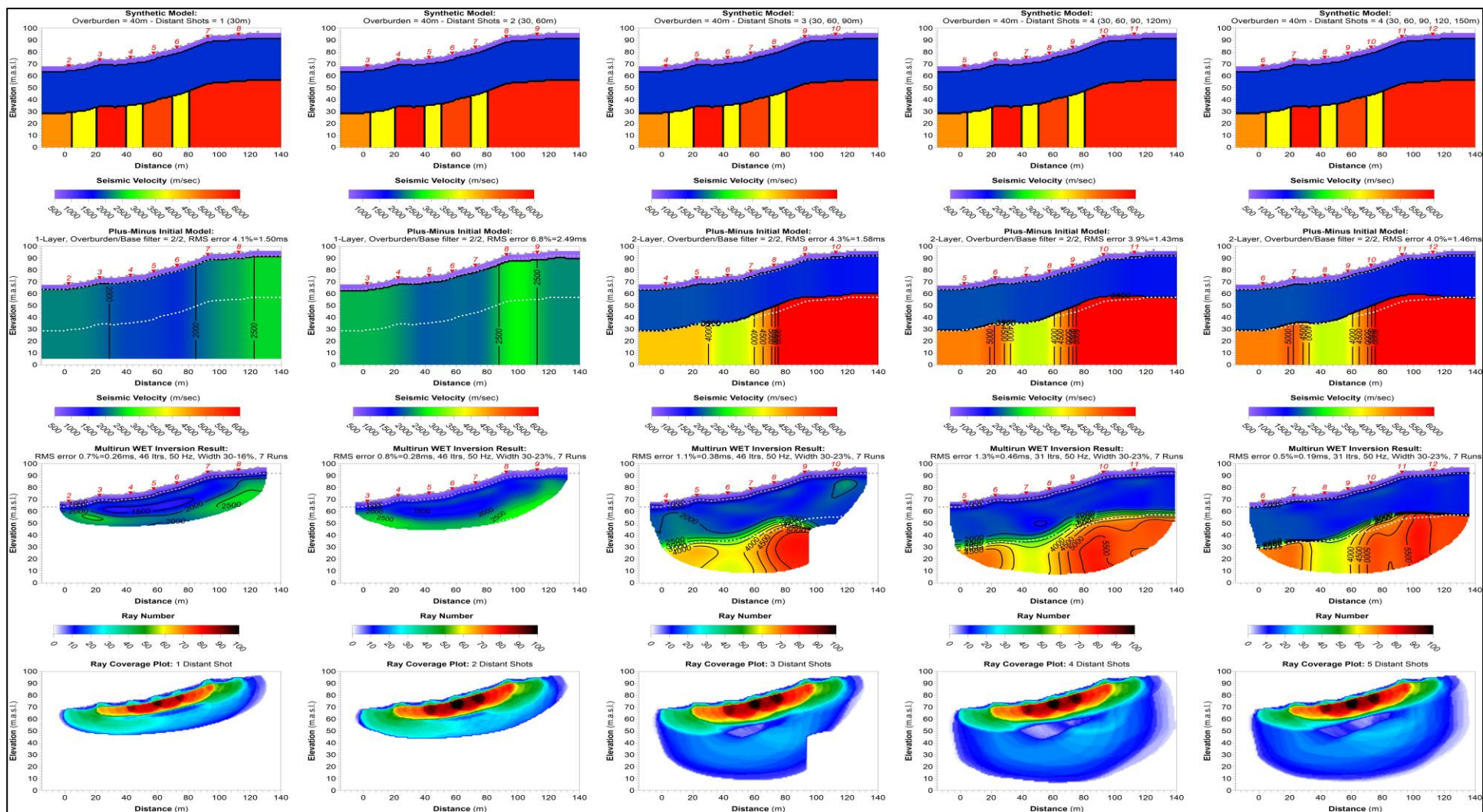


Figure 4: Modeling of the effect of off-end shots where the total soil thickness is 40 m. To the left: Dataset B1, distance shots at 30 m from the spread. No. 2: Dataset B2, distance shots at 30 m and 60 m from the spread. No. 3: Dataset B3, distance shots at 30 m, 60 m and 90 m from the spread. No. 4: Dataset B4, distance shots at 30 m, 60 m, 90 m and 120 from the spread and No. 5 (Right): Dataset B5, distance shots at 30 m, 60 m, 90 m, 120 m and 150 m from the spread. True layer interfaces are marked as a white dotted line.

### 4.3 Variations in off-end shots at 80 m soil cover

The results of the modelling with an 80 m soil cover are shown in Figure 5. The following section describes the images and present the fracture zone location/characterisation and the soil thickness/characterisation.

#### 4.3.1 Fracture zones location and characterisation

Neither Hagedoorn’s plus-minus-method nor the tomographic inversion can reveal the fracture zones from the synthetic model. The Dataset C4, with off-end shots 240 m away from the receiver spread, can see down to bedrock, but do not have the capability to resolve the velocity variations in bedrock.

#### 4.3.2 Soil thickness and characterisation

The starting model for Dataset C1, C2 and C3 (80 m soil cover, off-end shots at 60 m, 60 m + 120 m and 60 m + 120 + 180 m from end receivers) created with **Hagedoorn’s plus-minus-method**, do not reach down to bedrock (Figure 5). The off-end shots are too close to the receiver spread to be able to interpret the total soil thickness. For the Dataset C4 (Off-end shots at 60, 120, 180 and 240 m), it is possible to see the soil/bedrock interface, but the total soil thickness is a bit too low, in average 66.1 m or 82.6 % of the true total thickness (see Table 3). Again, this confirms the traditional rule of thumb, “off-end shots at least at a distance three times the total soil thickness away from the end receivers in the spread at both ends”.

All four datasets seem to give an acceptable image of the first layer thickness and velocity.

The **tomographic inversion** of the same profile shows a good image of the first soil layer with a velocity close to the true 600 m/s and thickness of ca. 5 m. The velocity in soil layer 2 is slightly above 1500 m/s, not far from the true velocity of 1600 m/s. None of the tomographic inverted datasets are able to reveal the soil/bedrock interface.

Table 4: Inverted soil velocities and thicknesses in meters and percent of true thickness from Dataset C, 80 m soil thickness.

| Dataset, True soil thickness | Inversion method | Velocity V1 (m/s) | Velocity V2 (m/s) | Total soil thickness (m) | Total soil thickness (%) | Mean soil thickness ± SDEV (m) | Mean soil thickness in % of true thickness |
|------------------------------|------------------|-------------------|-------------------|--------------------------|--------------------------|--------------------------------|--|
| C1, 80 m                     | Hagedoorn        | ≈ 600             | 1500-2500         | ?                        | ?                        | ?                              | ?  |
| C1, 80 m                     | Tomography       | ≈ 600             | 1500-2500         | ?                        | ?                        | ?                              | ?  |
| C2, 80 m                     | Hagedoorn        | ≈ 600             | 1500-2500         | ?                        | ?                        | ?                              | ?  |
| C2, 80 m                     | Tomography       | < 1000            | 1500-2500         | ?                        | ?                        | ?                              | ?  |
| C3, 80 m                     | Hagedoorn        | ≈ 600             | ≈ 1600            | ?                        | ?                        | ?                              | ?  |
| C3, 80 m                     | Tomography       | < 1000            | 1500-2000         | ?                        | ?                        | ?                              | ?  |
| C4, 80 m                     | Hagedoorn        | ≈ 600             | ≈ 1600            | 67 – 72                  | 84 - 90                  | 68.8 ± 1.6                     | 86.0 ± 2.1                                 |
| C4, 80 m                     | Tomography       | < 1000            | 1500-2000         | ?                        | ?                        | ?                              | ?  |

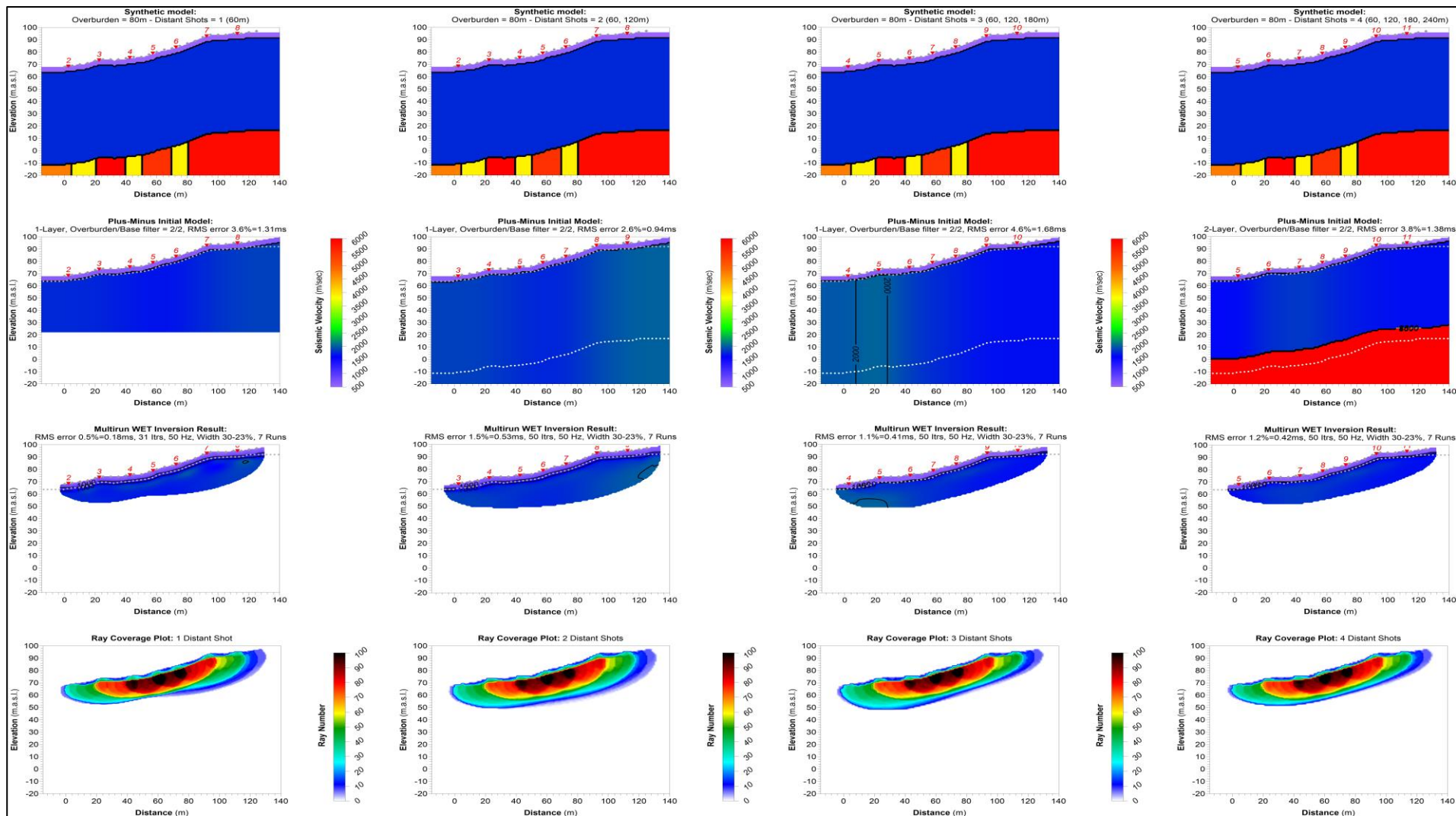


Figure 5: Modeling of the effect of off-end shots where the total soil thickness is 80 m. To the left: Dataset C1, distance shot at 60 m from the spread. No. 2: Dataset C2, distance shots at 60 m and 120 m from the spread. No. 3: Dataset C3, distance shots at 60 m, 120 m and 180 m from the spread and No. 4 (Right): Dataset C4, distance shots at 60 m, 120 m, 180 m and 240 from the spread. True layer interfaces are marked as white dotted line.

The ray coverages at the bottom of Figure 5 explains the penetration limitations. Too few rays are travelling into the bedrock, and an increased number of off-end shots provide not significant improvement. The tomographic inversion using Rayfract software is not able to use information from off-end shots.

#### 4.4 Effect of varying fracture zone velocity and depth extent

Interpretation with Hagedoorn's plus-minus method will reveal the top bedrock velocity variations as vertical zones. Westerdal (2003) showed that a 10 m deep depression in the bedrock surface could show up as a fracture zone with a velocity of 2500 m/s, that is interpreted as a zone with extremely bad rock quality. In most of our modelling so far (Tassis et al. 2017 and 2018), we have looked at vertical zones that have vertical extension deeper than the methods penetrating depth. To see if tomographic inversion can give a better image of undulations in bedrock topography, we have used our standard model and varied the depth extent of the fracture zone in the middle. At the same time, we have varied the velocities in the fractured zones. This is done for almost no soil cover (Dataset D) and with 20 m soil cover (Dataset E).

##### 4.4.1 Varying fracture zone velocity and depth extent with thin soil cover

For Dataset D1- D4 as shown in Figure 6, the geophone spacing is 5 m, the shot distance is 30 m and we have off-end shots 30 m and 60 m from end receivers in the spread. The soil thickness varies but is less than ca. 5 m. We model the results of variations in fracture zone velocity and depth extent with thin soil cover.

In Dataset D1 (Figure 6 to the left), the three fractures have full depth extent and velocities 3800 m/s, 2800 m/s and 2800 m/s, respectively. Dataset D2 is the same as Dataset D1 but the depth extent of fracture zone no. 2 is only 5 m. Dataset D3 is the same as Dataset D1 but the depth extent of fracture zone no. 2 is 10 m. Dataset D4 is the same as Dataset D1 but the depth extent of fracture zone no. 2 is 20 m. In general, all the inverted data locates all three fracture zones, and the positions are almost as in the synthetic model.

As previously seen (Tassis et al. 2017 and 2018), **Hagedoorn's plus-minus** method indicates all the three fracture zones in Dataset D1 and can characterise them. All fracture zones have a depth extent deeper than the penetration depth as already described. The fracture zone thickness and velocity fit the values in the synthetic model for Dataset D1 quite good. For Dataset D2, where depth extent of fracture zone no. 2 is 5 m, the interpreted velocity in the fracture zone is ca. 4200 m/s which is higher than the velocity in the synthetic model (2800 m/s). The velocity in the fracture zone no. 2 decreases gradually with depth: from 10 m and 20 m in Datasets D3 and D4. This means that a shallow depression in the bedrock topography will show up as deep vertical fracture zones with a higher velocity. This coincides with what Westerdal (2003) showed in his modelling.

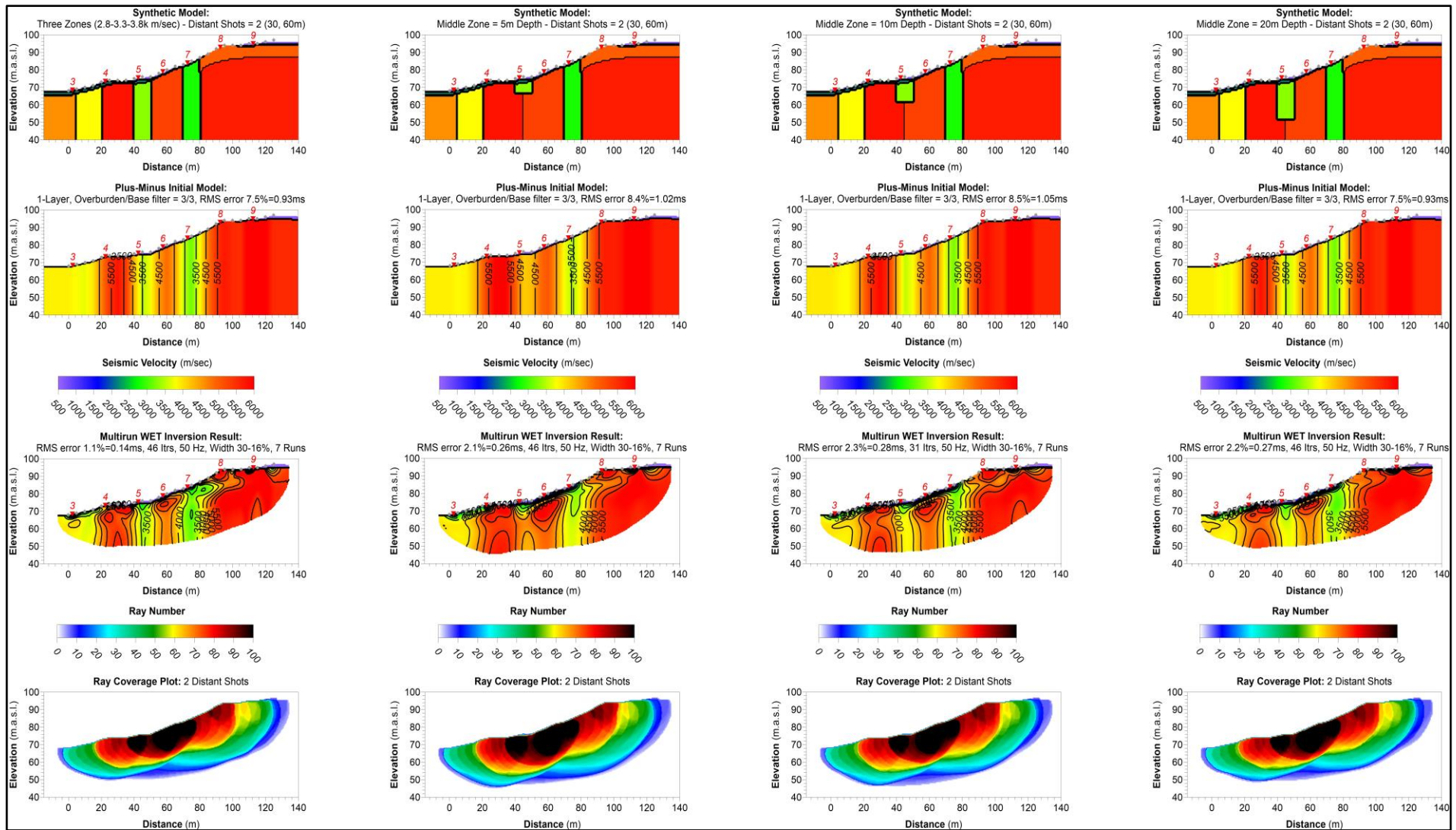


Figure 6: Modelling of the variations in fracture zone velocity and depth extent with thin soil cover. Right: Dataset D1(Full depth extent and velocities 3800 m/s and 2800 m/s), Dataset D2 (Same as Dataset D1 but 5 m depth extent of fracture zone 2), Dataset D3 (Same as Dataset D1 but 10 m depth extent of fracture zone 2) and Dataset D4 (Same as Dataset D1 but 20 m depth extent of fracture zone 2).



In the **tomographic inverted data**, the variation with depth of fracture zone no. 2 showed an interesting behaviour. In Dataset D2, the 5 m deep zone in the synthetic model shows up as a ca. 5 m deep depression with a value that fits the velocity in the synthetic model (2800 m/s). There is an artificial effect of low velocity at depth, but the velocity is quite high (4000 – 4500 m/s). In Dataset D3, where the depth extent of zone no. 2 is 10 m, this zone shows up as a combination of a ca. 5 m deep depression with almost correct velocity and a deeper extension with a ca. velocity of 3800 m/s (2800 m/s in the synthetic model). In Dataset D4, this fracture zone no. 2 is more pronounced.

This modelling shows that when the soil cover is thin, it is possible to reduce the false image effect of bedrock depression in Hagedoorn inversion by the tomographic inversion.

#### 4.4.2 Varying fracture zone velocity and depth extent with 20 m soil cover

In Figure 7, we show the modelling results of variations in fracture zone velocity and depth extent with a **20 m thick soil cover**. In Dataset E1, the three fractures have full depth extent and velocities 2800 m/s, 3800 m/s and 4800 m/s respectively. Dataset E2 is the same as Dataset E1 but the depth extent of fracture zone no. 2 is only 5 m. Dataset E3 is the same as Dataset E1 but the depth extent of fracture zone no. 2 is 10 m. Dataset E4 is the same as Dataset E1 but the depth extent of fracture zone no. 2 is 20 m. In addition to these three fracture zones, there is a zone with velocity 4600 m/s at the start of the profile. Velocities from 4600 to 5000 m/s is interpreted as “medium rock quality” (Table 13), and this zone is not regarded as the fractured zone.

As previously seen, **Hagedoorn’s plus-minus** method indicates all three fracture zones when the soil cover is 20 m, even zone no. 3 which here has a velocity of 4800 m/s, can be interpreted as good rock quality. However, all three zones are shifted ca. 5 m to the left. The low-velocity zone in the beginning of the profile, is merged with the 2800 m/s fracture zone to the right and given a false velocity between 3000 m/s and 3500 m/s. All fracture zones have a depth extent deeper than the penetration depth for the method, which is typical for Hagedoorn’s interpretation.

The interpreted velocity in zone no. 2 is between 3500 m/s and 4000 m/s in all datasets, and do not show the same variations as in Dataset D (Chapter 4.4.1). It is obvious that Hagedoorn’s automatic method is not giving as good images of the starting model than when soil is less thick.

In the **tomographic inverted data**, some of the artificial effects from Hagedoorn’s interpretation is inherited. The zones are shifted ca. 5 m to the left and zone 1 is merged with the low-velocity zone. The velocity variations in zone 2 we could see with thin soil cover (Figure 6, section 4.4.1), do not display in the same way. In Dataset E1, the velocity in zone 2 is ca. 3800 m/s as in the synthetic model. In Datasets E2, E3 and E4, where the depth extent is 5 m, 10 m and 20 m, the velocity is between 4000 m/s and 4500 m/s and do not show visible variations. The depth extent of the zone is also similar in the three models. It seems impossible to indicate the variations in the depth extent of zone no. 2 when the soil cover is 20 m or more. However, with a velocity between 4000 m/s and 4500 m/s, this false zone will not be considered as very problematic for tunnel excavation.

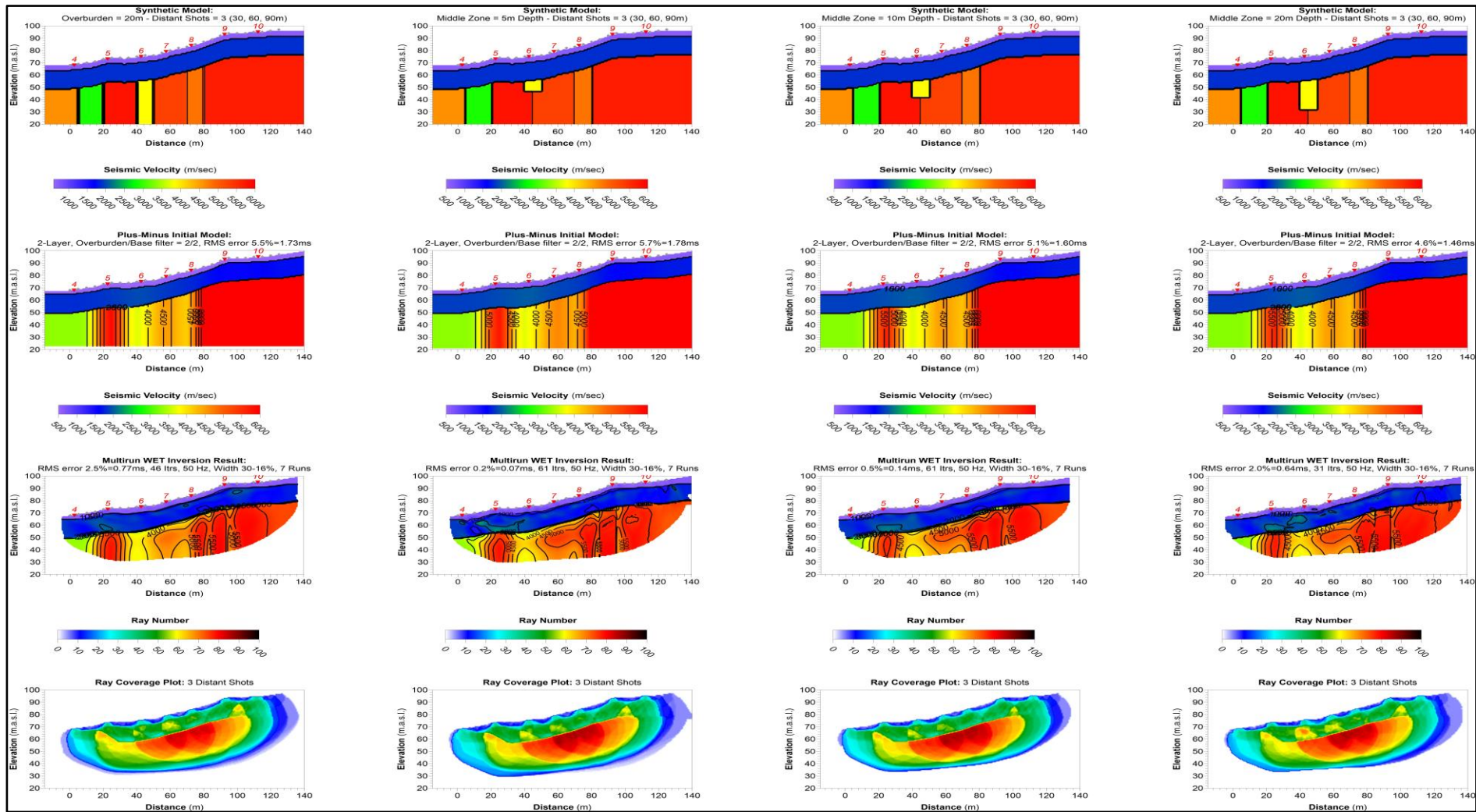


Figure 7: Modeling of the variations in fracture zone velocity and depth extent with 20 m soil cover. Right: Dataset E1 (Full depth extent and zone velocities 2800 m/s, 3800 m/s and 4800 m/s), Dataset E2 (Same as Dataset E1 but 5 m depth extent of fracture zone 2), Dataset E3 (Same as Dataset E1 but 10 m depth extent of fracture zone 2) and Dataset E4 (Same as Dataset E1 but 20 m depth extent of fracture zone 2).

Zone no. 3 with the velocity 4800 m/s show up at Dataset E1 but are more diffuse in Datasets E2, E3 and E4. It looks like the variation in the depth of zone 2 influences the possibility to view zone no. 3.

This modelling shows that when the soil cover is thick (20 m or more), the possibilities for fracture zone characterisation is less. We also see that the location can be more uncertain.

#### 4.5 Effect of a blind zone above bedrock on depth estimations

Blind zones or hidden layer appear when there is an increasing velocity with depth, but the actual layer is too thin to be detected (Reynolds 2011). Hidden layers are a problem in traditional refraction seismic interpretation, and it is interesting to see if this problem can be handled with tomographic inversion.

##### 4.5.1 Effect of blind zone at a 40 m thick two-layered soil cover

In Dataset F, shown in Figure 8, we look at the effect of a gradual increase of the thickness of a hidden layer, where the total soil thickness is 40 m. Geophone spacing is 5 m, shot distance is 30 m and there are off-end shots at 30, 60, 90 and 120 m from both end of the receiver spread. Dataset F1 has a homogenous soil thickness with a velocity 1600 m/s, possibly representing fine-grained marine sediments. In Datasets F2, F3 and F4 we introduce a hidden layer with thickness 5, 10 and 20 m above bedrock. The velocity in this is 2100 m/s which can represent a moraine layer. In bedrock there are three fracture zones (15, 10 and 10 m wide, velocity of 3800 m/s).

Neither the **Hagedoorn interpretation** nor the **tomographic inversion** is able to resolve the three fracture zones in bedrock (Figure 8). They are all merged into one ca. 30 m wide zone where the velocity is partly less than 3500 m/s in the Hagedoorn interpretation, and slightly higher (3500 – 3750 m/s) in the tomographic inversion. Due to the reduced velocity at the beginning of the profile (4600 m/s), the velocity left of the indicated fracture zone is slightly less than to the right of the fracture zone.

Both the **Hagedoorn method** and the **tomographic inversion** using Hagedoorn's interpretation as a starting model, indicate a close to correct velocity in the first soil layer ( $V_1 = 1600$  m/s). However, neither of these two methods can detect and characterise the hidden layer with velocity 2100 m/s above bedrock.

Also shown in Figure 8, is the interpreted total soil thickness from the models F1 to F4. The true soil thickness is indicated as a white dotted line. **The Hagedoorn inversion** of Dataset F1 fits pretty good to the true soil thickness, but there are some variations along the profile. As the thickness of the blind zone increases (Model F2, F3 and F4), the deviation from the true soil thickness also increases.

In the **tomographic inversion** of the models, the velocity increases gradually and does not give as sharp contrast as the Hagedoorn inversion. Here we have used the velocity contour 3000 m/s as an indicator of the bedrock surface. This fits quite well for model F1 where there is no blind zone. However, as the thickness of the blind zone increases, the deviation from the true total soil thickness increases also here.

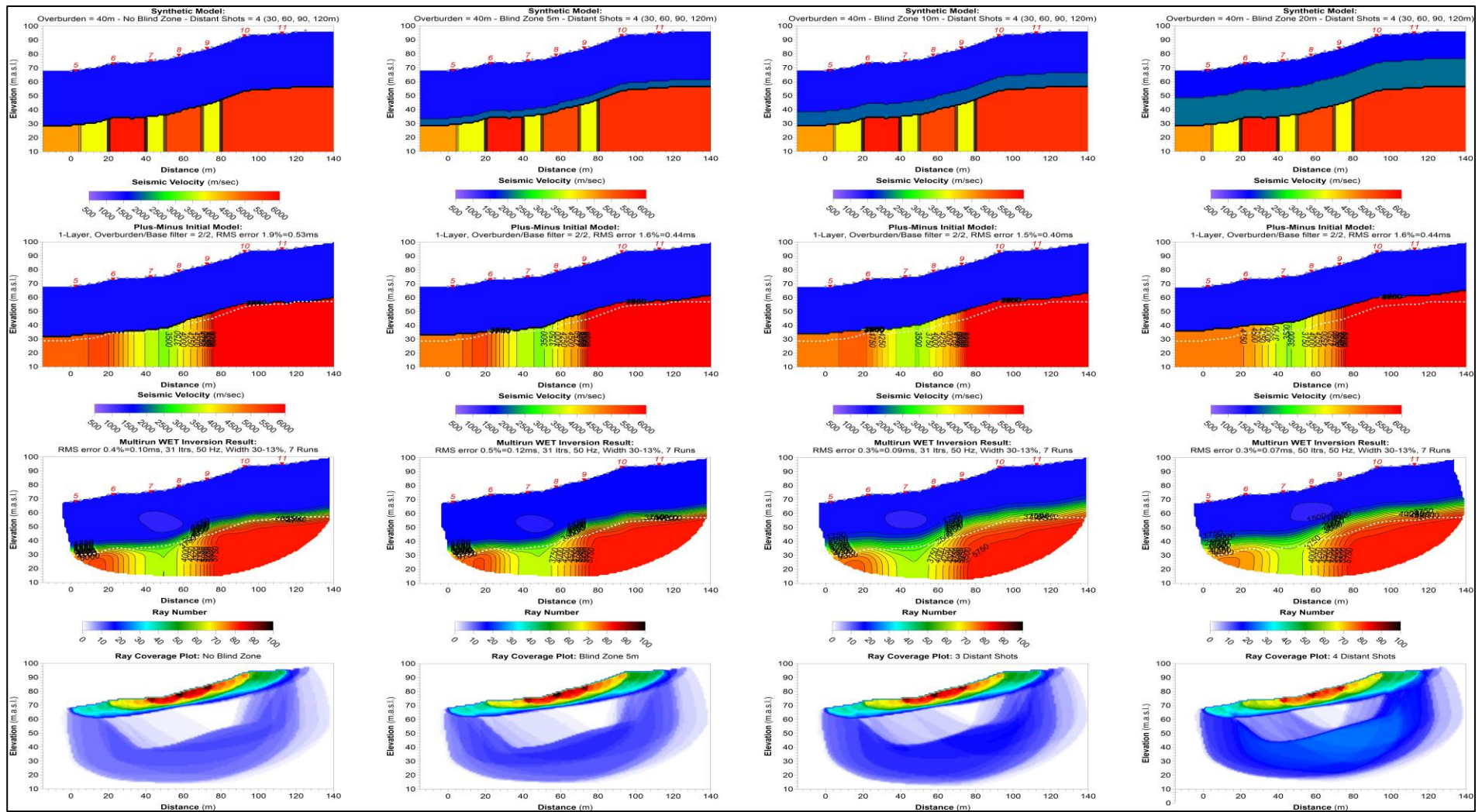


Figure 8: Modeling of variations of a “blind zone” in a 40 m soil cover above bedrock. From right: Dataset F1 (no blind zone,  $V_1 = 1600$  m/s), Dataset F2 (5 m thick blind zone,  $V_1 = 1600$  m/s,  $V_2 = 2100$  m/s). Dataset F3 (10 m thick blind zone,  $V_1 = 1600$  m/s,  $V_2 = 2100$  m/s) and to the right Dataset F4 (40 m thick blind zone,  $V_1 = 1600$  m/s,  $V_2 = 2100$  m/s). Velocity model in bedrock is the same as in Dataset B. True bedrock surface is indicated as white dotted line.

In Table 5, the deviations from true soil thickness are quantified for both inversion methods.

Table 5: Interpreted soil velocity and total soil thickness from Dataset F using Hagedoorn's method and tomographic inversion. The total soil thickness is 40 m in all models. Dataset F1 has a homogenous soil velocity 1600 m/s, Dataset F2 has a 5 m thick hidden layer with velocity 2100 m/s above bedrock. In Datasets F3 and F4, the thickness of the blind zone is 10 and 20 m.

| Dataset, Soil layer thicknesses (m) / Total soil thickness (m) | Inversion method | Interpreted Velocity V1 (m/s) | Total soil thickness variation (m) | Total soil thickness variation in (%) | Mean soil thickness $\pm$ SDEV (m) | Mean soil thickness in % of true thickness |
|--|------------------|-------------------------------|------------------------------------|---------------------------------------|------------------------------------|--|
| F1, 40 + 0 = 40  | Hagedoorn        | Ca. 1600                      | 35 - 40                            | 88 - 100                              | 37.0 $\pm$ 1.1                     | 92.5 $\pm$ 2.7                             |
| F1, 40 + 0 = 40  | Tomography       | 1500 - 1750                   | 35 - 39                            | 88 - 98                               | 37.5 $\pm$ 1.3                     | 93.8 $\pm$ 3.3                             |
| F2, 35 + 5 = 40  | Hagedoorn        | Ca. 1600                      | 33 - 37                            | 83 - 93                               | 35.7 $\pm$ 1.2                     | 89.2 $\pm$ 3.0                             |
| F2, 35 + 5 = 40  | Tomography       | 1500 - 1750                   | 33 - 39                            | 83 - 98                               | 36.5 $\pm$ 1.9                     | 91.3 $\pm$ 4.8                             |
| F3, 30 + 10 = 40   | Hagedoorn        | Ca. 1600                      | 33 - 36                            | 83 - 90                               | 34.5 $\pm$ 1.2                     | 86.3 $\pm$ 3.1                             |
| F3, 30 + 10 = 40   | Tomography       | 1500 - 1750                   | 33 - 40                            | 83 - 100                              | 35.6 $\pm$ 2.3                     | 89.1 $\pm$ 5.8                             |
| F4, 20 + 20 = 40   | Hagedoorn        | Ca. 1600                      | 30 - 39                            | 75 - 98                               | 32.9 $\pm$ 2.0                     | 82.2 $\pm$ 4.9                             |
| F4, 20 + 20 = 40   | Tomography       | 1500 - 1750                   | 30 - 36                            | 75 - 90                               | 32.9 $\pm$ 1.9                     | 82.2 $\pm$ 4.7                             |

As can be seen in Table 5, the soil velocity is ca. 1600 m/s for the **Hagedoorn method**, and in the interval 1500 m/s to 1750 m/s for the **tomographic inversion**. None of the methods indicate velocities around 2100 m/s from the blind zones. In general, the interpreted soil thickness is less than the true total soil thickness as seen in Figure 8. Since none of the inversion methods is not able to detect the blind zone, a too low velocity is used in the inversion which results in a too low soil thickness. However, also the model F1 without a blind zone show a too low soil thickness.

To get an idea of the deviations from the true total thickness, the interpreted thickness is estimated at the start point of the profile, under each shotpoint and at the endpoint of the profile, altogether eight to nine points at each profile. Here,  $V = 3000$  m/s isoline was used as indicator of top bedrock. For the Hagedoorn interpretation of model F1 without the blind zone, the total soil thickness varies between 35 m and 40 m (37 m  $\pm$  1.5 m) and on average, the total soil thickness is 92.5 % of the true thickness. The tomographic inversion using the Hagedoorn interpretation as starting model improves these values by about 1.3 %.

Increasing thickness of the blind zone decreases the interpreted average soil thickness, and for Dataset F4, the interpreted values are 82.2 % of the true depth for both the Hagedoorn interpretation and the tomographic inversion.

### Summary.

Neither of the two methods (Hagedoorn and the tomographic inversion) could resolve the fracture zones in bedrock under a 40 m thick soil cover. However, the three zones were merged into one with a total thickness of ca. 30 m and velocity from less than 3500 m/s to ca. 3800 m/s, not far from the total true values in the synthetic model.

The inversions gave a good image of soil velocity in layer no. 1 (1600 m/s). As expected, the Hagedoorn method was not able to detect the hidden layer, and the interpreted soil thickness proved to be too low. The Tomographic inversion using the Hagedoorn interpretation as starting model, did not improve the interpreted soil thickness significantly. All interpreted total soil thicknesses (depth to bedrock) were lower than the true depth, 82.2 % for Dataset F4 with a 20 m thick hidden layer.

#### 4.5.2 Effect of blind zone at a 40 m thick three-layered soil cover

Dataset G shown in Figure 9, is equal the Dataset F except for a five meters thick soil layer ( $V= 600$  m/s) at the top. Shallow low-velocity layers may have a high impact on total soil thickness (depth to bedrock) interpretations. As expected, an additional shallow low-velocity soil layer, does not improve the ability to resolve the fracture zones in bedrock. However, it did not make it worse either.

The interpreted velocities in soil layer no. 1 (600 m/s) and soil layer no. 2 (1600 m/s) are good for the Hagedoorn interpretation. The tomographic inversion shows a more undulating velocity in soil layer no. 2. Partly, the velocity here is less than 1500 m/s and occasionally less than 1250 m/s. The tomographic inversion indicates a velocity inversion (lower velocity in deeper layer) which is physically impossible to discover with traditional refraction seismic interpretation including Hagedoorn's method used here. However, in this case this is an artificial (false) effect. None of the interpretations performed here are able to detect the third soil layer (true velocity 2100 m/s) which can be a blind zone (hidden layer). Even with a thickness of 20 m (Dataset G4) this layer was not detected.

Apparently, the interpreted thickness of the top layer is close to the true thickness for both methods (Figure 9). However, as shown in Table 6, the thickness of this layer is occasionally less than 50 % of the true thickness. Here, layer thicknesses are estimated at the start and the end of the profile and under each shooting points. In this interpretation (both Hagedoorn and tomographic inversion), the velocity contour  $V=750$  m/s were used as indicator for the interface between soil layer one and two, which seems to be correct in some places but too low in others. The tomographic inversion reduces the thickness of this first layer compared with the Hagedoorn's inversion.

Table 6: Interpreted soil layer thicknesses and total soil thickness (depth to bedrock) from Dataset G using Hagedoorn's method and tomographic inversion. The total soil thickness is 40 m in all models. Dataset G1 has two soil layers ( $V1 = 600$  m/s and  $V2=1600$  m/s) velocity, Dataset G2 has in addition a 5 m thick blind zone with velocity 2100 m/s above bedrock. In Datasets G3 and G4, the thickness of the blind zone is 10 and 20 m.

| Dataset, Soil layer thicknesses and Total thickness (m) | Inversion method | Mean thickness layer 1 $\pm$ SDEV (m) | Thickness layer 1 / True thickness (%) | Thickness layer 2 $\pm$ SDEV (m) | Thickness layer 2 / True thickness $\pm$ SDEV (%) | Depth to bedrock / SDEV (m) | Depth to bedrock / True depth (%) $\pm$ SDEV (%) |
|---|------------------|---------------------------------------|--|----------------------------------|---|-----------------------------|--|
| G1, 5+35+0=40   | Haged.           | 4.0 $\pm$ 0.3                         | 80.0 $\pm$ 5.0                         | 32.6 $\pm$ 1.9                   | 93.0 $\pm$ 5.4                                    | 36.6 $\pm$ 1.8              | 91.4 $\pm$ 4.5                                   |
| G1, 5+35 +0=40  | Tomo             | 2.6 $\pm$ 0.5                         | 51.3 $\pm$ 9.9                         | 34.8 $\pm$ 2.3                   | 99.5 $\pm$ 6.6                                    | 37.4 $\pm$ 2.2              | 93.4 $\pm$ 5.5                                   |
| G2, 5+30 +5=40  | Haged.           | 2.8 $\pm$ 0.4                         | 56.7 $\pm$ 8.7                         | 31.7 $\pm$ 2.0                   | 105 $\pm$ 6.6                                     | 34.6 $\pm$ 2.0              | 86.4 $\pm$ 5.0                                   |
| G2, 5+30 +5=40  | Tomo             | 2.3 $\pm$ 0.7                         | 45.0 $\pm$ 14                          | 33.4 $\pm$ 1.6                   | 111 $\pm$ 5.3                                     | 35.6 $\pm$ 1.7              | 89.1 $\pm$ 4.2                                   |
| G3, 5+25 +10=40   | Haged.           | 3.6 $\pm$ 0.5                         | 71.1 $\pm$ 9.3                         | 31.0 $\pm$ 1.5                   | 124 $\pm$ 5.9                                     | 34.6 $\pm$ 1.5              | 86.4 $\pm$ 3.8                                   |
| G3, 5+25 +10=40   | Tomo             | 2.3 $\pm$ 0.5                         | 45.0 $\pm$ 9.3                         | 32.6 $\pm$ 1.7                   | 130 $\pm$ 6.4                                     | 34.8 $\pm$ 1.8              | 86.9 $\pm$ 4.4                                   |
| G4, 5+15 +20=40   | Haged.           | 3.6 $\pm$ 0.5                         | 71.1 $\pm$ 9.3                         | 28.8 $\pm$ 1.5                   | 192 $\pm$ 10                                      | 32.3 $\pm$ 1.4              | 80.8 $\pm$ 3.5                                   |
| G4, 5+15 +20=40   | Tomo             | 2.6 $\pm$ 0.5                         | 51.3 $\pm$ 9.9                         | 29.8 $\pm$ 1.5                   | 199 $\pm$ 8.7                                     | 32.4 $\pm$ 1.2              | 80.9 $\pm$ 3.0                                   |

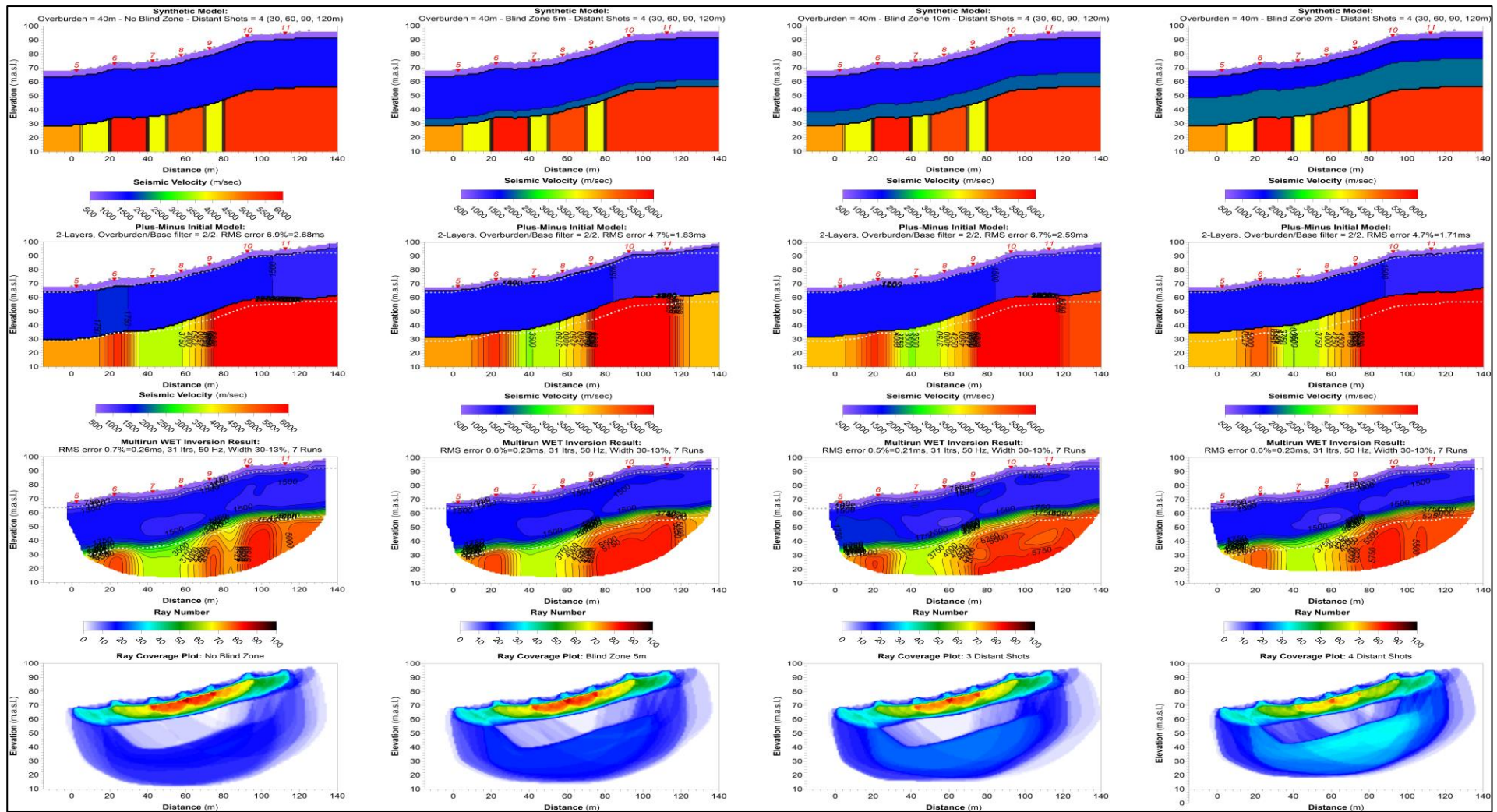


Figure 9: Modeling of variations of a “hidden layer” in a 40 m soil cover including a 5 m thick top layer of dry sediment (600 m/s) above bedrock. From right: Dataset G1 (no blind zone,  $V_1 = 600$  m/s,  $V_2 = 1600$  m/s), Dataset G2 (5 m thick blind zone,  $V_1 = 600$  m/s,  $V_2 = 1600$  m/s and  $V_3 = 2100$  m/s). Dataset G3 (10 m thick blind zone,  $V_1 = 600$  m/s,  $V_2 = 1600$  m/s and  $V_3 = 2100$  m/s) and to the right Dataset G4 (20 m thick blind zone,  $V_1 = 600$  m/s,  $V_2 = 1600$  m/s and  $V_3 = 2100$  m/s). Velocity model in bedrock is the same as in Dataset B. True layer interfaces is indicated as white dotted line.

In Datasets G1 and G2 the interpreted thickness of the second soil layer ( $V_2 = 1600$  m/s) is acceptable, 93 % to 111 % of true thickness. For Dataset G3 and G4, the interpreted thickness of this layer is unacceptable (124 % to 199 %). However, the total soil thickness (depth to bedrock) is close to the results from Dataset F where the thin dry soil layer with velocity 600 m/s is missing.

## **Summary of Hagedoorn interpretations**

The interpreted velocity of the first two layers is close to the true value. However, no method could detect the third layer. An indicated velocity inversion is an artificial effect.

The interpreted thicknesses of the first soil layer are partly far too low. Most likely a higher velocity isoline should have been used as indicator. The interpreted thickness of soil layer 2 is far too high for the Dataset G3 and G4 since the third soil layer ( $V=2100$  m/s) is not detected. The total soil thickness, however, is almost the same as for Dataset F, but unfortunately too low for all Datasets.

## **4.6 Alternative inversion of a two- and three-layered soil model**

To see the quality of depth to bedrock interpretations with alternative inversions, Datasets F and G are also interpreted using the DeltatV method for generating the starting model. In addition, Dataset G is interpreted by the company IMPAKT Geofysik AB using an alternative software for seismic tomography, DW Tomo (vers. 9.15 from Geogiga) and by manual calculation by Björn Toresson (Impakt Geofysik).

### **4.6.1 NGU inversion using Rayfract and the DeltatV method**

Hagedoorn's method is based on manual crossover point picking or a semiautomatic midpoint break picking (Intelligent Resources 2019a and b). In this way, the operators can influence on the interpretation by using their own knowledge. This may be a good solution for the inversion process, but at the same time this can limit the freedom to discover problems as velocity inversion and hidden layers. To overcome this pitfall, the DeltatV method can be used to generate the starting model for the inversion. DeltatV can be performed fully automatic where the starting model is without any influence from the operator and can also be controlled completely by the operator.

The DeltatV method generates a 2D starting velocity model which is less suited as a standalone inversion model. Earlier modelling has shown that this method is not optimal for locating and characterising fracture zones in bedrock (Tassis et al. 2017 and 2018), and in this work we concentrate on depth to bedrock interpretation. Both the DeltatV starting model and the tomographic inverted model show up with a velocity gradient towards the depth. This means that the inverted velocity depth sections must be interpreted to find the depth to bedrock.

### **Inversion of Dataset F using the DeltatV method.**

The DeltatV inversion of Dataset F, is shown in Figure 10.



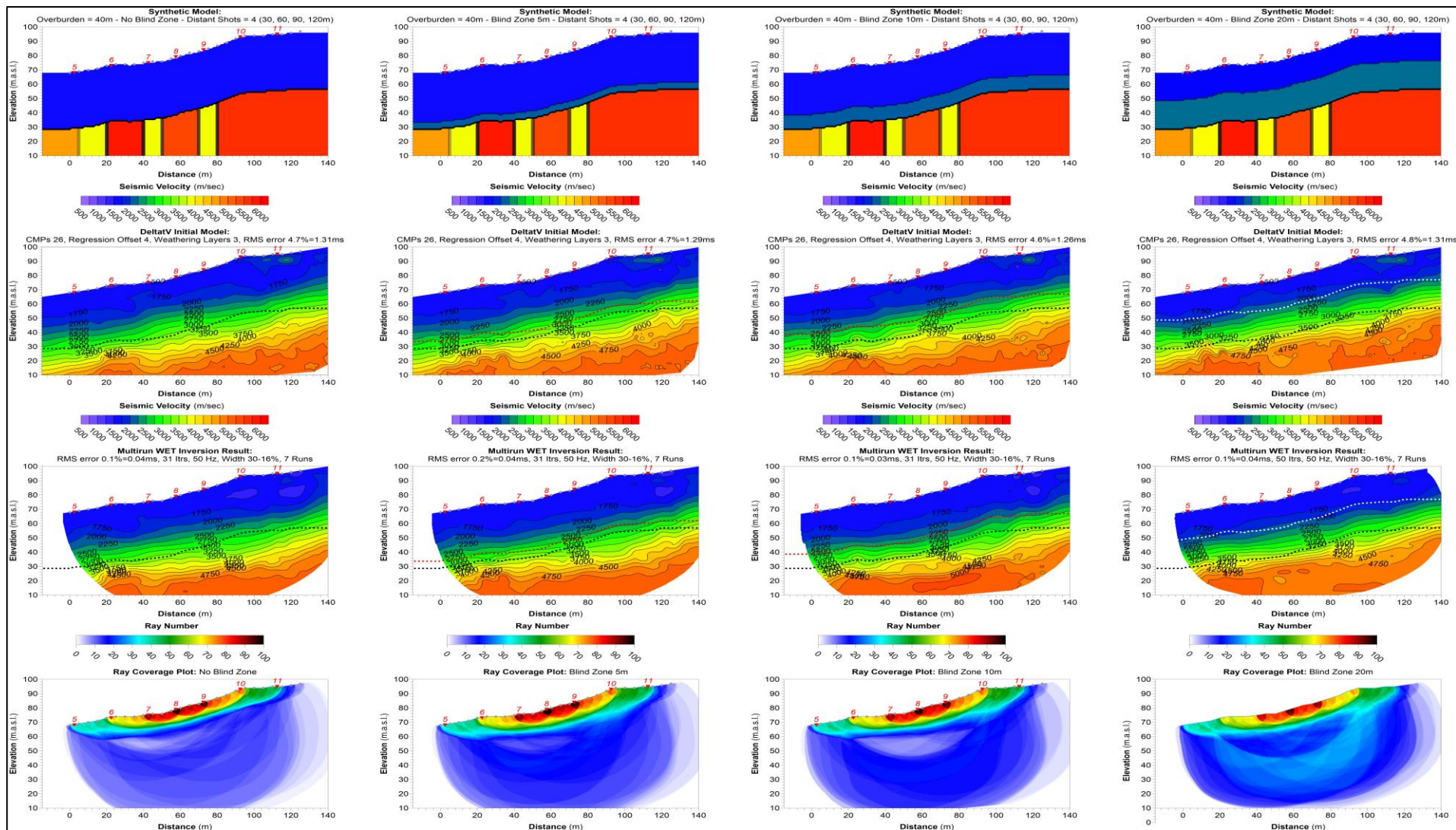


Figure 10: Modeling of variations of a “hidden layer” in a 40 m soil cover using the DeltatV starting model (Model F). The synthetic models are the same as in Figure 8. From left: no hidden layer, then a 5 m, 10 m and a 20 m thick hidden layer (velocity 2100 m/s under layer with velocity 1600 m/s). True layer interfaces are indicated as white, red or black dotted lines.

The **DeltatV** and the **tomographic inversion** using the DeltatV starting mode, shows a gradient velocity section. Since the depth to bedrock is known from the synthetic model, it is possible to see at which velocity isoline the bedrock appears in the interpreted gradient velocity section. As seen in Figure 10, rather than following a particular isoline, the bedrock undulates within an isoline interval. These isolines are read from the gradient velocity sections at the starting point, ending point and at all shot points in between, altogether eight or nine points along the profiles. Table 7 shows the isoline interval (minimum and maximum values) for both the starting model and the tomographic inversion, and the average of all readings including the standard deviation for the different velocity sections. The spreading of these isoline-bedrock crossings varies between 2750 m/s and 4000 m/s, which gives a significant standard deviation.

Table 7: Velocity isoline where true bedrock is located for DeltatV starting model and tomographic inversion using this as starting model and multirun assumed best inversion procedure. Dataset F.

| Dataset | Method           | Isoline Min- Max (m/s) | Average Isoline (m/s) | SDEV Isoline (m/s) |
|---------|------------------|------------------------|-----------------------|--------------------|
| F1      | Starting model   | 2750 - 3500            | 3083                  | 214                |
| F1      | Tomographic inv. | 2600 - 3500            | 3050                  | 288                |
| F2      | Starting model   | 2750 - 3600            | 3200                  | 276                |
| F2      | Tomographic inv. | 2750 - 3500            | 3263                  | 318                |
| F3      | Starting model   | 3000 - 3750            | 3390                  | 253                |
| F3      | Tomographic inv. | 2800 - 3750            | 3288                  | 300                |
| F4      | Starting model   | 3000 - 4200            | 3528                  | 347                |
| F4      | Tomographic inv. | 3050 - 4000            | 3575                  | 330                |
| Average |                  |                        | 3297                  | 291                |

The average isoline values vary between 3050 m/s (tomographic inversion of Dataset F1) and 3575 m/s (tomographic inversion of Dataset F4). In a real situation, we do not know if we have a hidden layer or how thick it is. This means that without additional information, an isoline must be chosen as an indicator of bedrock. In this study,  $V = 3250$  m/s was chosen as a representative value for all the models. Using this isoline as indicator of bedrock interface, depth to bedrock is interpreted as shown in Table 8.

Table 8: DeltatV interpretation, starting model and tomographic inversion of Dataset F. Total soil thickness is 40 m. Model F1 has no hidden layer, F2 a 5 m thick layer, F3 a 10 m thick layer and F4 a 20 m thick hidden layer. Depth to bedrock using isoline  $V=3250$  m/s as top bedrock indicator.

| Dataset | Method DeltatV | Depth interval (m) | Depth interval in percent of true depth (%) | Average Depth $\pm$ SDEV (m) | Deviation from true depth (%) |
|---------|----------------|--------------------|---|------------------------------|-------------------------------|
| F1      | Starting model | 39 - 48            | 98 - 120                                    | 42.1 $\pm$ 2.8               | 105 $\pm$ 7.0                 |
| F1      | Tomo-inversion | 38 - 50            | 95 - 125                                    | 41.9 $\pm$ 4.1               | 105 $\pm$ 10                  |
| F2      | Starting model | 36 - 47            | 90 - 118                                    | 40.3 $\pm$ 3.3               | 101 $\pm$ 8.3                 |
| F2      | Tomo-inversion | 36 - 48            | 90 - 120                                    | 40.8 $\pm$ 3.5               | 102 $\pm$ 8.8                 |
| F3      | Starting model | 35 - 42            | 88 - 105                                    | 37.2 $\pm$ 2.3               | 93 $\pm$ 5.7                  |
| F3      | Tomo-inversion | 35 - 46            | 88 - 115                                    | 39.5 $\pm$ 3.6               | 99 $\pm$ 9.1                  |
| F4      | Starting model | 34 - 40            | 85 - 100                                    | 36.7 $\pm$ 2.2               | 92 $\pm$ 5.6                  |
| F4      | Tomo-inversion | 35 - 42            | 88 - 105                                    | 37.9 $\pm$ 2.6               | 95 $\pm$ 6.5                  |
| Average | All            |                    |   | 39.5 $\pm$ 2.1               | 99 $\pm$ 5.2                  |

As can be seen in Table 8, interpreted depth to bedrock using isoline  $V=3250$  m/s as an indicator, reveal great variations, from 34 m to 48 m. As a percentage, this varies from 85 % to 120 % of the true depth to bedrock. In many cases, this is unacceptable

values. However, the average depth to bedrock is much more compressed, from 36.7 m to 42.1 m of true depth. As a percentage, the average depth to bedrock varies from 92 % to 105 %, which is within the traditional accuracy demands of +/- 10 %.

The **tomographic inversion** improves the results when a hidden layer is present (5 m thick in Dataset F2, 10 m in Dataset F3 and 20 m in Dataset F4). The velocity analysis and soil characterisation is more challenging. The first soil layer with velocity 1600 m/s, which can be fine graded water-saturated marine sediments (clay and silt), show velocity variations from 1500 m/s to ca. 3000 m/s, even 3750 m/s in the tomographic inversion. According to tabulated values this can be interpreted as anything from water-saturated fine graded sediments to crystalline bedrock of very poor quality.

The second layer, which can be a hidden moraine layer with velocity 2100 m/s, show velocities that vary between ca. 2600 m/s to ca. 4000 m/s. The geologic interpretation of this can be anything from extremely hard moraine or extremely poor rock quality to bedrock of bad rock quality.

The material that lies below the true soil-bedrock interface shows a velocity distribution from 2750 m/s to more than 5000 m/s (extremely poor rock quality to very good rock quality). The DeltatV interpretation creates a velocity section that cannot be used to characterise the soil and the bedrock quality.

Using the **DeltatV** starting model and the **tomographic inversion** using this, we find signs of vertical fracture zones in bedrock. However, the velocity sections show up with a horizontal gradient velocity distribution that can be interpreted as weathered bedrock which is not the case in the synthetic model.

Although it has a different velocity distribution than in the synthetic model, the DeltatV starting model shows an RMS error of about 4.7 % (1.3 mS) and for the tomographic inversion these numbers are 0.1 – 0.3 % (0.04 ms), which is a very good model fitting (Figure 10). This is a good example of how several models can fit the data fairly good, but still not show the true model.

### **Inversion of Dataset G using the DeltatV method.**

The DeltatV inversion of Dataset G is shown in Figure 11. Both the DeltatV starting model and the tomographic inversion show a gradient velocity distribution. An interpretation of soil-bedrock interface is needed, and it is not obvious where this interface is located. The same kind of analysis where soil-bedrock interface appears as for Dataset F is performed for Dataset G.

Table 9 shows the isoline interval (minimum and maximum values) where true top bedrock is located, and the average of 9 readings along the line including the standard deviation. The spreading of these isoline-bedrock crossings varies between 2750 m/s and 4000 m/s, which gives a significant standard deviation.

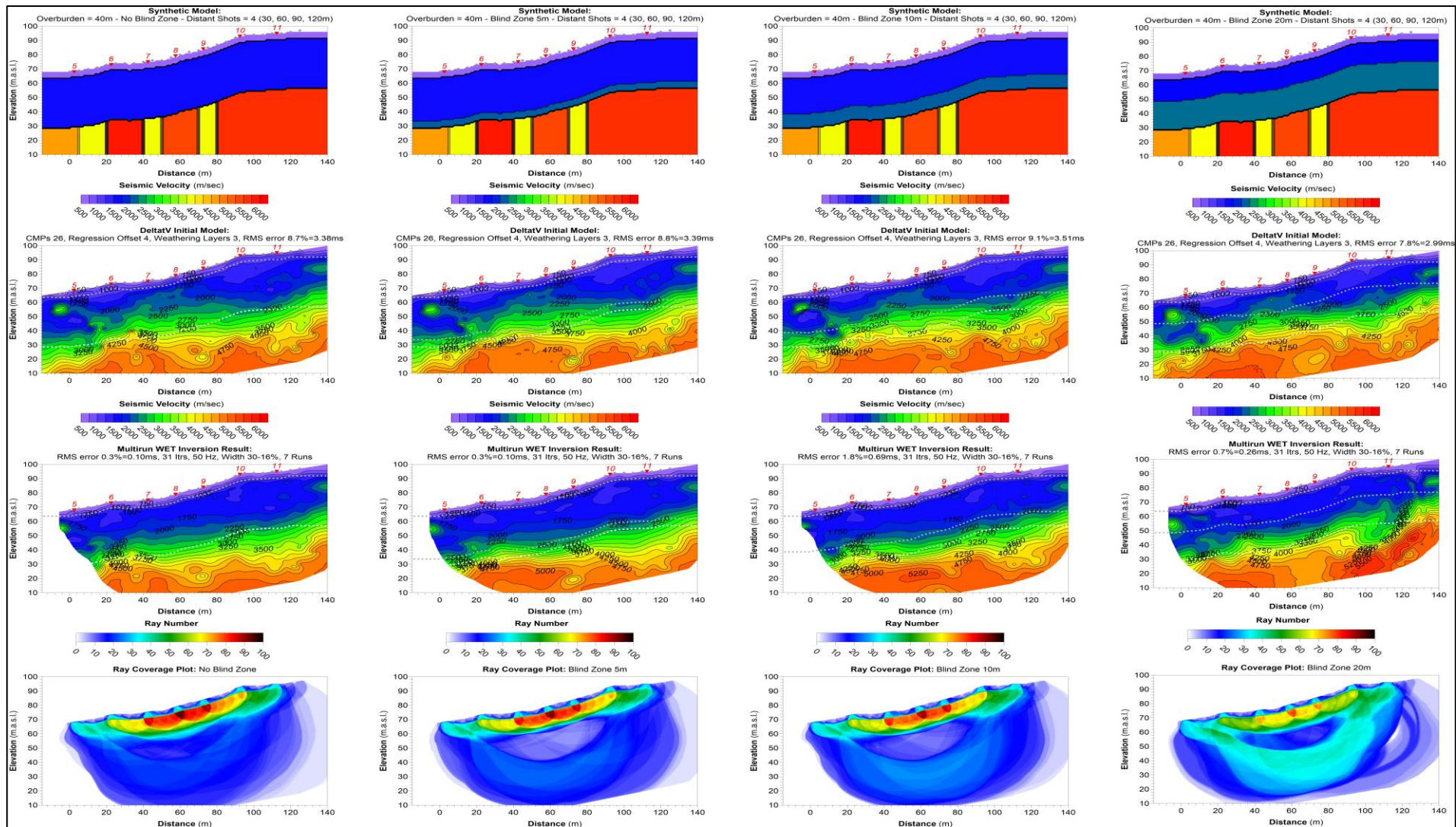


Figure 11: Modeling of variations of a "hidden layer" in a 40 m soil cover using the DeltatV starting model. The synthetic models are the same as in Dataset G (Figure 9). On top there is a dry soil layer with velocity of 600 m/s. From left: no hidden layer, then a 5 m, 10 m and a 20 m thick hidden layer (velocity 2100 m/s under layer with velocity 1600 m/s). True layer interfaces are indicated as white dotted lines.

Table 9: Velocity isoline where true bedrock is located for DeltatV starting model and tomographic inversion using this as starting model and multirun assumed best inversion procedure for Dataset G.

| Dataset | Method           | Isoline Min- Max (m/s) | Average Isoline (m/s) | SDEV Isoline (m/s) |
|---------|------------------|------------------------|-----------------------|--------------------|
| G1      | Starting model   | 2400 - 3500            | 3033                  | 448                |
| G1      | Tomographic inv. | 2500 - 3500            | 3000                  | 433                |
| G2      | Starting model   | 2500 - 3800            | 3111                  | 533                |
| G2      | Tomographic inv. | 2500 - 3750            | 3063                  | 449                |
| G3      | Starting model   | 2750 - 3750            | 3250                  | 451                |
| G3      | Tomographic inv. | 2750 - 3750            | 3175                  | 381                |
| G4      | Starting model   | 2800 - 4400            | 3667                  | 641                |
| G4      | Tomographic inv. | 2500 - 4500            | 3381                  | 596                |
| Average |                  |                        | 3210                  | 492                |

The average isoline values vary between 3000 m/s (tomographic inversion of Dataset G1) and 3667 m/s (DeltatV starting model of Dataset G4) which is a wider spread than for the Dataset F (Table 7). However, the average isoline is somewhat lower than for Dataset F. Isoline  $V=3250$  m/s as indicator for soil-bedrock interface was also here chosen as a representative value for all the models. Using this isoline as indicator of soil-bedrock interface, depth to bedrock is as shown in Table 10.

Table 10: DeltatV interpretation (starting model and tomographic inversion) of Dataset G. Total soil thickness is 40 m. Depth to bedrock using isoline  $V=3250$  m/s as top bedrock indicator.

| Dataset | Method      | Depth interval (m) | Depth interval in percent of true depth (%) | Average Depth $\pm$ SDEV (m) | Deviation from true depth (%) |
|---------|-------------|--------------------|---|------------------------------|-------------------------------|
| G1      | Start model | 37 - 50            | 93 - 125                                    | 42.1 $\pm$ 4.8               | 105 $\pm$ 12                  |
| G1      | Tomoinv.    | 38 - 50            | 95 - 125                                    | 43.4 $\pm$ 4.7               | 109 $\pm$ 12                  |
| G2      | Start model | 34 - 49            | 85 - 123                                    | 40.5 $\pm$ 5.0               | 101 $\pm$ 13                  |
| G2      | Tomoinv.    | 37 - 48            | 93 - 120                                    | 42.1 $\pm$ 4.4               | 105 $\pm$ 11                  |
| G3      | Start model | 31 - 49            | 78 - 123                                    | 38.8 $\pm$ 6.0               | 97 $\pm$ 15                   |
| G3      | Tomoinv.    | 35 - 47            | 88 - 118                                    | 40.9 $\pm$ 4.4               | 102 $\pm$ 11                  |
| G4      | Start model | 32 - 43            | 80 - 108                                    | 37.6 $\pm$ 3.6               | 94 $\pm$ 9                    |
| G4      | Tomoinv.    | 33 - 50            | 83 - 125                                    | 39.8 $\pm$ 4.9               | 100 $\pm$ 13                  |
| Average | All         |                    |   | 40.6 $\pm$ 1.9               | 102 $\pm$ 4.8                 |

As shown in Table 10, interpreted depth to bedrock using  $V=3250$  m/s as a top bedrock indicator, reveal even more significant variations than for Dataset F (Table 8), from 31 m to 50 m. As a percentage this varies from 78 % to 125 % of the true depth to bedrock. It is obvious that introducing an extra soil layer (more complicated models), give greater uncertainty in the depth to bedrock interpretations. However, the **average depth to bedrock** is much more compressed, from 37.6 m to 43.4 m. As a percentage, the average depth to bedrock varies from 94 % to 109 %, which is within the traditional accuracy demands of  $\pm 10$  %. The tomographic inversion increases the deviation from true bedrock depth by 4 to 6 %, giving a less accurate result for Dataset G1 and G2 (none or thin hidden layer) but more accurate for a thicker hidden layer (Dataset G3 and G4 where the hidden layer is 10 and 20 m thick).

The velocity analysis is challenging also for this dataset, both for the **DeltatV starting** model and the **tomographic inverted** model. The first soil layer with velocity 600 m/s

falls in a velocity interval from 500 m/s to 1250 m/s which can be interpreted as dry soil and partly water-saturated soil.

The second soil layer with velocity 1600 m/s, which can be water saturated sediments (clay-silt-sand-gravel), show velocity variations from 700 m/s to ca. 3000 m/s. According to tabulated values this can be interpreted as anything from dry fine graded sediments to crystalline bedrock of extremely poor quality.

The third soil layer, which can be a hidden moraine layer with a velocity of 2100 m/s, shows velocities that vary between ca. 1500 m/s to ca. 4500 m/s. The geologic interpretation can include the presence of water-saturated sediments, extremely hard moraine and/or extremely poor to poor rock quality (see Table 13).

The material that lies below the true soil-bedrock interface shows a velocity distribution from 2750 m/s to more than 5500 m/s (extremely poor rock quality to very good rock quality). It is obvious that the DeltatV interpretation creates a velocity section that cannot be used to characterise the soil and the bedrock quality. This inversion does not give any sign of the three fracture zones in bedrock.

#### 4.6.2 IMPAKT inversion of Dataset G using software from Geogiga

The tomographic inversion of Dataset G using the Geogiga software is shown in Figure 12. The inversion is performed by Roger Wisén at IMPAKT Geofysik AB using two different parameter settings. Synthetic starting models are shown at the top. As a comparison, the Rayfract multirun tomographic inversion using Hagedoorn starting model is shown at the bottom (NGU inversion).

The way the inversions are performed here, gives no indication of fractured zones in bedrock. Whether or not this is possible using Geogiga software is not tested. The Geogiga inversion show a smoother velocity gradient that is parallel to the layers in the synthetic model compared with the Rayfract DeltatV inversion.

Table 11 shows the velocity isoline interval (minimum and maximum values) where true top bedrock appears. True bedrock in the sections lies between isolines 2750 m/s and 4000 m/s, which is slightly less than for the Rayfract DeltatV inversions.

Table 11: Velocity isoline interval where true bedrock is located. An average velocity including standard deviation is calculated at 8 position along the lines for Geogiga tomographic inversion performed by IMPAKT Geofysik, same data as Dataset G, two different inversion settings.

| Dataset | Method           | Isoline Min- Max (m/s) | Average Isoline (m/s) | SDEV Isoline (m/s) |
|---------|------------------|------------------------|-----------------------|--------------------|
| G1.1    | Tomographic inv. | 2750 – 3000            | 2881                  | 128                |
| G2.1    | Tomographic inv. | 2800 – 3250            | 3063                  | 148                |
| G3.1    | Tomographic inv. | 2950 - 3400            | 3194                  | 124                |
| G4.1    | Tomographic inv. | 3250 - 4000            | 3538                  | 334                |
| G1.2    | Tomographic inv. | 2750 – 3050            | 2856                  | 121                |
| G2.2    | Tomographic inv. | 2800 – 3250            | 3056                  | 143                |
| G3.2    | Tomographic inv. | 3000 – 3300            | 3147                  | 134                |
| G4.2    | Tomographic inv. | 3250 - 3900            | 3531                  | 244                |
| Average |                  |                        | 3158                  | 260                |

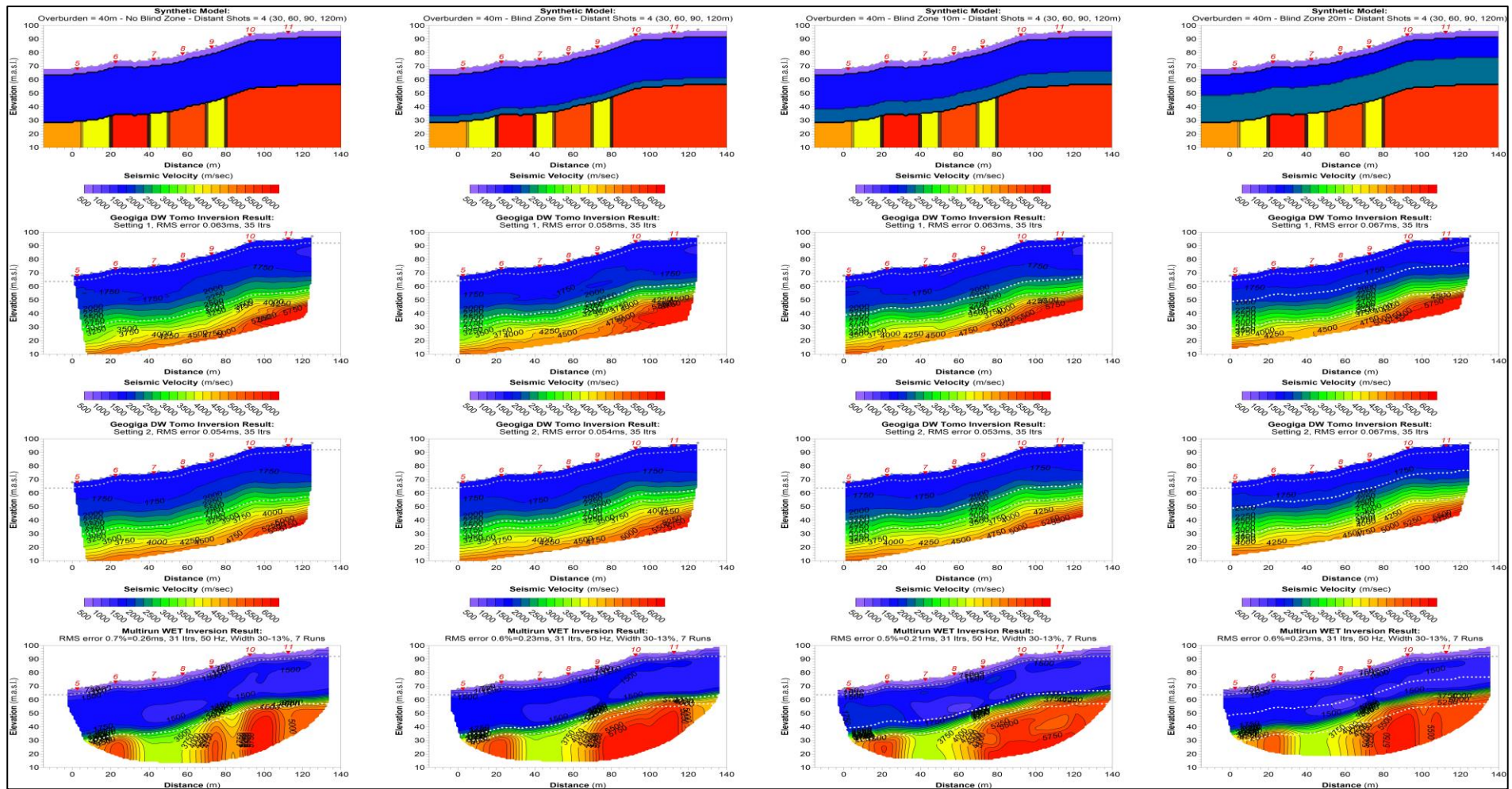


Figure 12: Modelling of variations of a “hidden layer” in a 40 m soil cover using the Geogiga software, Dataset G. The synthetic models are shown as the top image. Then follows Geogiga tomographic inversions with two different parameters. For comparison, the tomographic multirun inversions using Hagedoorn starting model are shown at the bottom. The model consists of a dry soil layer with velocity 600 m/s as a top layer, and the second layer can be wet sediments ( $V=1600$  m/s). From left: no hidden layer (G1), then a 5, 10 and a 20 m (G2 – G4) thick hidden layer (velocity 2100 m/s under layer with velocity 1600 m/s). The true layer interfaces are indicated as white dotted lines.

Average velocities, including the standard deviations, at the soil bedrock interface are calculated at 8 points along the lines (at the shotpoints and at the endpoints). On average, the best isoline as bedrock indicator for inversion setting 1 is ca. 2880 m/s for Dataset G1, ca. 3060 m/s for Dataset G2, ca. 3190 m/s for Dataset G3 and ca. 3540 m/s for Dataset G4. For inversion setting 2, there is a minor decrease in these values. The standard deviation for these numbers varies from 124 m/s to 334 m/s and represents the true bedrock undulation within the velocity isolines intervals. The Geogiga tomographic inversion show up almost the same variation as the Rayfract DeltatV tomographic inversion, increasing hidden layer thickness makes the true soil-bedrock interface to appear at increasing velocity isolines.

Where to interpret the depth to bedrock is dependent on the geologic model. No fixed velocity isoline can be used as a standard value. In our interpretation, we have used the velocity isoline  $V=3250$  m/s as bedrock indicator. This value is too high for the G1 model (no hidden layer) and too low for the G4 model (20 m thick hidden layer). Despite this, all average depth to bedrock interpretations in Table 12 lie within the traditional accuracy uncertainties of  $\pm 10\%$ , and on average, the interpreted depth to bedrock is 100 % of true depth. The use of individual velocity indications for depth to bedrock for the four models could have further improved the results.

Table 12: Geogiga interpretation of depth to bedrock performed by IMPAKT Geofysik of Dataset G. Total soil thickness is 40 m. Depth to bedrock using isoline  $V=3250$  m/s as top bedrock indicator, two different inversions settings (G1.1, G1.2 and so on).

| Dataset | Method Geogiga | Depth interval (m) 8 points | Depth interval in percent of true depth (%) | Average Depth $\pm$ SDEV (m) 8 points | Deviation from true depth (%) |
|---------|----------------|-----------------------------|---|---------------------------------------|-------------------------------|
| G1.1    | Tomo-inv.      | 40.0 – 43.1                 | 100 - 108                                   | $41.6 \pm 1.1$                        | $104 \pm 2.7$                 |
| G2.1    | Tomo-inv.      | 37.9 – 43.1                 | 95 - 108                                    | $40.5 \pm 1.5$                        | $101 \pm 3.9$                 |
| G3.1    | Tomo-inv.      | 39.0 – 44.1                 | 98 - 110                                    | $40.5 \pm 1.6$                        | $101 \pm 4.1$                 |
| G4.1    | Tomo-inv.      | 35.9 – 39.0                 | 90 - 98                                     | $37.8 \pm 1.4$                        | $94 \pm 3.5$                  |
| G1.2    | Tomo-inv.      | 41.0 – 44.1                 | 103 - 110                                   | $42.4 \pm 1.2$                        | $106 \pm 3.0$                 |
| G2.2    | Tomo-inv.      | 39.0 – 43.1                 | 90 - 108                                    | $41.0 \pm 1.3$                        | $103 \pm 3.4$                 |
| G3.2    | Tomo-inv.      | 39.0 – 43.1                 | 90 - 108                                    | $40.2 \pm 1.3$                        | $101 \pm 3.3$                 |
| G4.2    | Tomo-inv.      | 34.9 – 41.0                 | 87 - 103                                    | $37.2 \pm 2.2$                        | $93 \pm 5.4$                  |
| Average | All            | 34.9 – 44.1                 | 87 - 110                                    | $40.2 \pm 1.5$                        | $100.4 \pm 3.7$               |

#### 4.6.3 IMPAKT traditional interpretation of Dataset G1

For comparison, the results we have achieved by software controlled inversion of Dataset G1, IMPAKT Geofysik has performed traditionally layered earth Hagedoorn interpretation of this data. The work is performed by senior geophysicist Björn Toresson and was a blind test where the interpreter had no information about the synthetic model. Unfortunately, there has not been time to interpret Datasets G2, G3 and G4 in the same way. The topics fracture zone detection and characterisation, thickness of soil layers and characterisation of soil layers are all of interest.

The result of the traditional interpretation of Dataset G1 is shown in Figure 13, together with the synthetic model, and NGUs tomographic inversion using Hagedoorn starting model. Bedrock velocity were calculated using several geophone (average velocity) and more detailed using first incoming event at individual geophones.



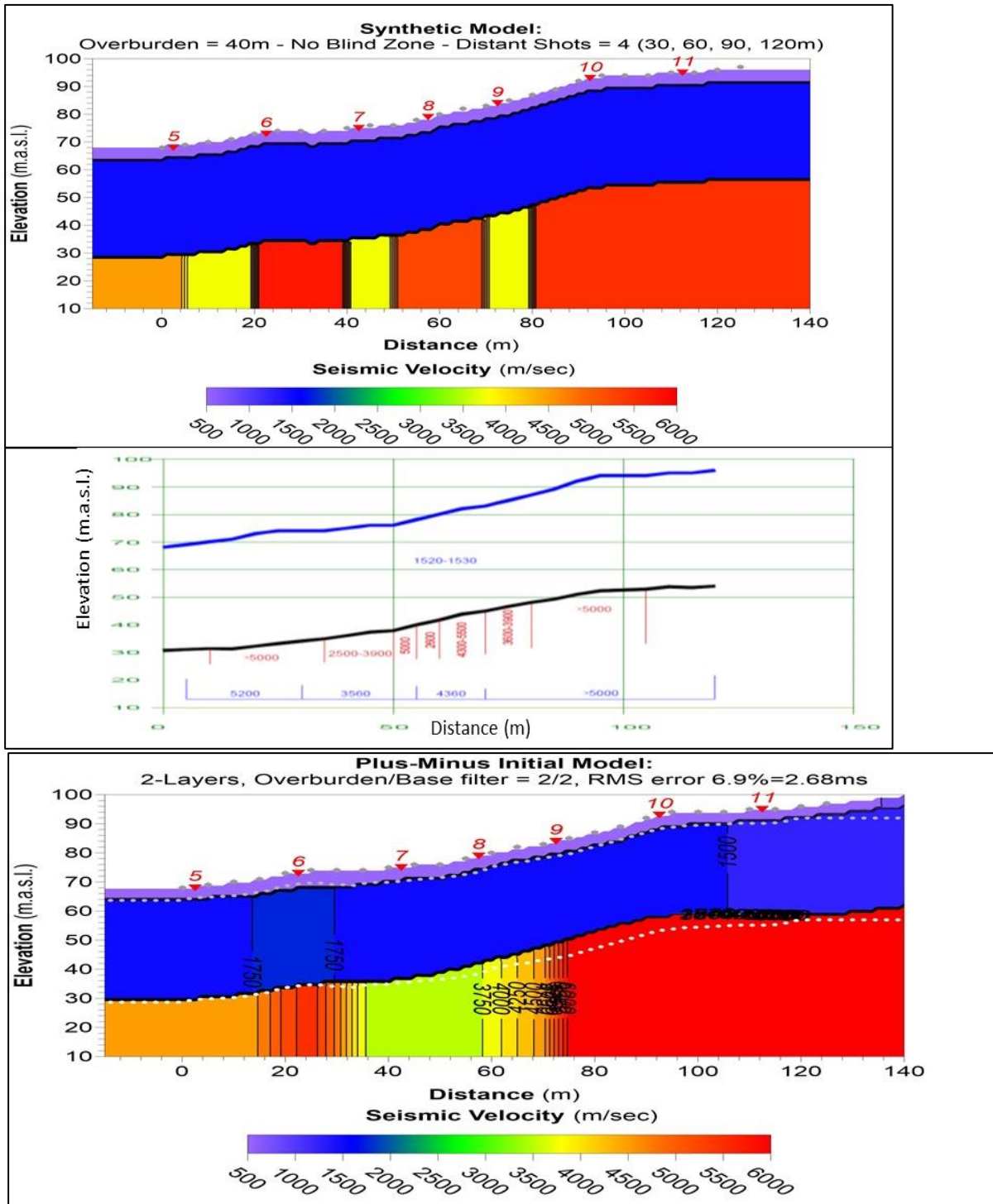


Figure 13: Traditional Hagedoorn interpretation of Dataset G1. On top, the synthetic model, in the middle the traditional interpretation and for comparison the automatic Rayfract Hagedoorn inversion at the bottom. Blue numbers in the traditional interpretation represents average bedrock velocity analyses while red numbers represent detailed interpretation between each individual receiver.

### Detection and characterisation of fracture zones

In the average bedrock velocity analyses (blue numbers in the middle, Figure 13) indicate a ca. 40 m wide low velocity zone with two different velocities, 3560 and 4360 m/s. This average velocity interpretation is more like the Rayfract Hagedoorn

inversion by NGU (at the bottom) where the three low velocity zones representing fractured bedrock, merge into one wide velocity zone.

The more detailed interpretation, however, indicates three low velocity zones, first (to the left) a ca. 20 m wide zone of a velocity 2500 – 3900 m/s, then a ca. 5 m wide zone of a velocity 2600 m/s and then a ca. 10 m wide zone of a velocity 3600 – 3900 m/s. The latter is very close to the third zone in the synthetic model, both in position, in width and in velocity span (3800 m/s in synthetic model). The zone in the middle is too thin and the velocity is lower than in the synthetic model. The zone to the left is somewhat thicker (15 m in the synthetic model) and the velocity is partly lower than in the synthetic model (3800 m/s). This can be an effect of the reduced velocity in the beginning of the synthetic model (4600 m/s) which is not indicated in the traditional interpretation. The detailed traditional interpretation gives a good image of the three fracture zones in the synthetic model.

### **Bedrock depth and characterisation of soil material**

The total depth to bedrock at 10 points along the profile show up values from 37.7 m to 42.2 m. In average this is 40.1 m and a standard deviation of 1.5 m, which is a perfect match with the total thickness in the synthetic model.

In the traditional velocity model, layer no. 1 (600 m/s) is not detected and the velocity in the detected soil single layer was slightly too low (1520 – 1530 m/s vs. 1600 m/s in the synthetic model). The automatic Hagedoorn interpretation picked up the low velocity layer at the top, but indicated a velocity in layer 2 which is mostly lie between 1500 m/s and 1750 m/s and partly > 1750 m/s. In a real situation, layer 1 in the Hagedoorn interpretation would be interpreted as dry material as indicated in the synthetic model. At both methods, the next layer would be interpreted most likely as water saturated clay-sand-gravel, but also loose compacted moraine (Table 14).

## **5. DISCUSSION**

NGU has chosen to use the software Rayfract (Intelligent Resources 2019a) and Hagedoorn's method for inversion of refraction seismic data. In this chapter, the results obtained on the topics such as detection and characterisation of fracture zones in bedrock, depth to bedrock and characterisation of soil material are discussed. In order to explore other routines, the DeltatV method within Rayfract is tested. With some help from IMPAKT Geofysik, software from Geogiga and traditional interpretation are tested for mapping and characterisation of soil. The discussion of this modelling of synthetic data should be compared with analysis of real refraction seismic data from the project "Crossing of the Romsdalsfjord" (Rønning et al. 2020).

### **5.1 Detection and characterisation of fracture zones in bedrock**

NGU has previously studied detection and characterisation of fracture zones using Rayfract software (Tassis et al. 2017 and 2018, Rønning et al. 2016, 2019a and 2019b).). In the present work, the effect of soil thickness, distance to off-end shots and variation in fracture zone velocity and depth extent are studied.

In the discussion on rock mass quality, we adopt the same velocity intervals used by the Norwegian Public Road administration (Table 13, from Rønning et al. 2020). These intervals are valid for basement rocks in Norway but may change in other bedrock types.

Table 13: Rock mass class, p-wave velocity, and rock characterisation (From Rønning et al. 2020).

| Rock class | P-wave velocity (m/s) | Rock characterisation (description) |
|------------|-----------------------|-------------------------------------|
| A/B        | > 5000                | Good to very good rock quality      |
| C          | 5000 - 4600           | Medium rock quality                 |
| D          | 4600 - 4000           | Poor rock quality                   |
| E          | 4000 - 3000           | Very poor rock quality              |
| F          | 3000 – 2000           | Extremely poor rock quality         |
| G          | < 2000                | Exceptionally poor rock quality     |

### 5.1.1 Effect of increasing soil cover thickness using Hagedoorn's method

In previous NGU work to locate and characterise fracture zones in bedrock, the effect of off-end shots was not fully explored when the soil thickness increased. In the present study, capabilities and limitations of fracture zone detection and characterisation is modelled for total soil thickness of 20 m, 40 m and 80 m. A complex model containing three 10 to 15 m thick fractured zones with velocity 3800 m/s and other bedrock velocity variations are used. Earlier modelling has shown that these zones could be located and characterised well under a 1 m to 5 m thick soil cover (Tassis et al. 2017 and 2018).

With a **total soil cover of 20 m** and only one off-end shot 30 m away from the receiver spread on both sides, only two of the fracture zones were mapped. The third merged with a zone with velocity 4600 m/s and showed up as ca. 30 m thick zone with a velocity slightly above 4500 m/s (bad rock quality). Increased number of off-end shots, 60 m and 90 m from both ends of the receiver spread, improved the image of the fractured zones, but still, only two of the zones were mapped. The total thickness of these was ca. 35 m which is close to the real total thickness of the three zones. The velocity varied from ca. 3500 m/s to ca. 4000 m/s (ie. very bad rock quality) which also fits with the original fracture zone velocities. The tomographic inversion of these models gave a similar result, but the image was a bit more diffuse. Localisation and characterisation of fracture zones under a 20 m thick soil cover using Rayfract and Hagedoorn's method is possible both in the starting Hagedoorn model and by tomographic inversion. However, a simplified model may be the result.

At a **total soil thickness of 40 m**, the Hagedoorn interpretation does not reach down to bedrock unless the off-end shots are 90 m or more away from the receiver spread. In this case, the three fracture zones are merged into one zone with thickness of ca. 35 m and an internal velocity about 3800 m/s (very bad rock quality) as in the synthetic model. Off-end shots at 120 m and 150 m from the receiver spread improved the image slightly, especially for the tomographic inversion. Location and characterisation of fracture zones under a 40 m thick soil cover using Hagedoorn's method and tomographic inversion is still possible, but an even more simplified model showed up. The horizontal resolution for bedrock characterisation diminished, and it is still unclear

whether shorter receiver distance and/or other inversion routines can improve the resolution. In order to solve this, more modelling is necessary.

The modelling results obtained with 20 m and 40 m soil cover indicate that in a real situation using Rayfract software and Hagedoorn's method, a thick fractured zone under a soil cover of about 20 m or more, might be caused by several thinner fractured zones.

At a total **soil thickness of 80 m**, the Hagedoorn interpretation does not reach down to bedrock unless the off-end shots are 240 m or more away from the receiver spread. This fits well with the traditional rule of thumb; that is, off-end shots should be more than three times the soil thickness away from the receiver spread. None of the three fracture zones were identified, which means the capability for localisation and characterisation of fracture zones is lost using the automatic Hagedoorn method.

Previous modelling (Tassis et al. 2018) has shown that to get a good image of a fracture zone, a receiver distance equal to one-third of the zone is necessary. This requirement is not fulfilled in this modelling where receiver distance is 5 m and fracture zone width is 10 m.

Detection and characterisation of fracture zones in bedrock using Rayfract software is more challenging as soil thickness increases. To be able to get information from bedrock, the distance to off-end shots should be three times the depth to bedrock.

#### 5.1.2 Detection and characterisation of fracture zones using the DeltatV method

NGU has previously concluded that tomographic inversion using the **DeltatV starting model** is not as efficient for fracture zone detection and characterisation as the Hagedoorn starting model (Tassis et al. 2017 and 2018). In the present work with a total soil overburden of 40 m (Figure 11 and Figure 12), there is no indication of fractures zones using the DeltatV method, despite some responses at the Hagedoorn method. There is no reason for changing the first conclusion.

#### 5.1.3 Effect of fracture zone velocity and depth extent

To see the effect of fracture zone velocity and depth extent, synthetic data were inverted using Rayfract and starting model generated with Hagedoorn's method for models with a 1 m to 5 m thick soil cover and a 20 m thick soil cover.

The modelling of the synthetic data with a **thin soil cover** (1 – 5 m), showed a really good image of the fracture zones (Figure 6). As expected for the **Hagedoorn inversion**, it was not possible to get information on the depth extent of the fractured zones. However, the fracture zone with 5 m depth extent showed a higher velocity (ca. 4500 m/s) than in the synthetic model (2800 m/s). Fracture zones with velocity 4500 m/s is often interpreted as bad rock quality but not far from medium rock quality (> 4600 m/s, Table 13). In the tomographic inversion, the fracture zone with 5 m depth extent showed up as a ca. 5 m deep depression in bedrock surface with minor velocity anomaly underneath. The example shows that a minor depression in bedrock surface, that shows up in the Hagedoorn inversion as a deep vertical zone, can be

processed away using **the tomographic inversion** to provide a better characterisation of the rock quality. This effect was also seen in the real data interpretation of refraction seismic data from the “Romsdalsfjord” project (Rønning et al. 2020). Tomographic inversion is one way to overcome Westerdahl’s problems (2003), as pinpointed in his theoretical studies on depressions in bedrock surface when the soil cover is thin.

If the depth extent of the bedrock depression increases to 10 m and 20 m, the depression shows up as a deep, clear, vertical fracture zone in the Hagedoorn starting model. The velocity is higher (better rock quality) than in the synthetic model. The tomographic inversion further increased the velocity (3500 m/s to 4000 m/s), and the depression shows up as a fracture zone with better rock quality (2800 m/s and extremely bad rock quality in the synthetic model).

In **Dataset E, with a total soil thickness of 20 m**, the fracture zone velocity in the synthetic model varied more (2800 m/s, 3800 m/s and 4800 m/s) and the depth extent of the second zone was 5, 10, 20 m and full depth extent. In the latter, the velocity in the zones varied slightly in the **Hagedoorn inversion** compared with the velocities in the synthetic model. The first 2800 m/s zone merged with the low velocity in the first part of the profile, got wider (ca. 25 m) but with a higher velocity (ca. 3200 m/s). The second zone with velocity 3800 m/s showed up as ca. 10 m wide zone with a velocity close to 3800 m/s, nearly the same as in the synthetic model. The third zone, where the synthetic model has a velocity 4800 m/s, shows up as a ca. 10 m wide zone with a velocity slightly less than 4500 m/s. In the **tomographic inversion**, this zone appears less pronounced with velocity mostly between 4500 m/s and 5000 m/s. Again, this is an example of a false zone in the Hagedoorn interpretation (artificial effect) that can be altered to a zone more like the one in the synthetic model.

Under 20 m soil cover, the effect of variation in fracture zone depth extent is less than in the thin soil cover example. In the **Hagedoorn interpretation**, the responses are almost equal despite variations in depth extent from 5 to 10 and 20 m. The only clear effect here is at zone no. 3 which appears to be wider and with slightly lower velocity. In the **tomographic inversion**, the velocity sections do not vary much with increasing depth extent of fracture zone two. The ability to characterise fracture zones under a 20 m soil cover is less than under a thinner soil cover.

#### 5.1.4 Fracture zone detection and characterisation with different methods

Fracture zone detection and characterisation using the Geogiga software failed (Figure 12). It is still unclear if another processing procedure can give a better result. More modelling is needed.

The traditional refraction seismic interpretation, with a 40 m soil cover were able indicate fractured zones in the same manner as the automatic Hagedoorn’s method using the Rayfract software. However, a **more detailed interpretation** looking at velocity variation in bedrock between each receiver, showed a fairly good image of the fracture zones in the synthetic model. All three fracture zones were indicated, but there were minor discrepancies in the thickness, in the internal velocity and in the positions. Tassis et al. (2018) showed that to be able to give a good image of a

fracture zone, a perfect receiver distance should be one third of the fracture zone thickness. In this case, this is not fulfilled.

In Table 14, we summarise the ability to detect and characterise fracture zones in bedrock using different inversion techniques.

Table 14: The ability to detect and characterise fractured zones in bedrock using Rayfract software (Hagedoorn and DeltatV including tomographic inversion using these as starting model), Geogiga tomographic inversion and traditional Hagedoorn manual interpretation.

| Method                | Detect | Characterise | Comments                            |
|-----------------------|--------|--------------|-------------------------------------|
| Hagedoorn             | Yes    | Yes          | Good at thin soil cover             |
| Hagedoorn tomo        | Yes    | Yes          | Good at thin soil cover             |
| DeltatV               | No     | No           | Not with the procedure used here    |
| DeltatV tomo          | No     | No           | Not with the procedure used here    |
| Geogiga tomo          | No     | No           | Not with the procedure used here    |
| Traditional Hagedoorn | Yes    | Yes          | Good at thin and thicker soil cover |

**Automatic Hagedoorn** inversion using the Rayfract software can give fairly good images of fracture zones when the soil thickness is thin (Tassis et al 2017 and 2018, this report). The resolution is less when there is a thicker soil cover. **Tomographic inversion** using the Hagedoorn starting model can also detect and characterise fracture zones in bedrock and in addition reduce artificial effects created with the Hagedoorn method. The way the DeltatV and the tomographic inversion using this as starting model is performed here, is not able to give a good image of fracture zones in bedrock. To explore this, further modelling is needed. The same can be said about the Geogiga tomographic inversion performed by IMPAKT Geofysik. The traditional interpretation of refraction seismic seems to be the best option for detection and characterisation of fracture zones in bedrock. The initial model used in this work (Figure 2) was originally interpreted manually by Morgan Wåle (2009). The most detailed traditional interpretation performed by Bjørn Toresson (IMPAKT Geofysik) were able to resolve the three fractured zones under a 40 m soil cover.

Under thick soil cover (> 20 m), location and characterisation of fracture zones should be performed by traditional manual interpretation.

## 5.2 Depth to bedrock calculations

NGU has used several methods to calculate depth to bedrock using the Rayfract software; Hagedoorn's method, DeltatV method and tomographic inversion using these interpretations as starting model. In addition, the company Impakt Geofysik has used software from Geogiga to perform tomographic inversion, and one Dataset (G1) is interpreted using traditional Hagedoorn's method.

### 5.2.1 Quality of depth to bedrock calculations using Hagedoorn's method

NGU has previously studied the inversion of synthetic data with a thin soil layer and got quite good results regarding soil thickness and velocity (Tassis et al. 2017 and 2018). In the present work, we have looked at total soil thicknesses of 20, 40 and 80

m. We have also introduced a hidden layer (blind zone) with varying thickness above bedrock. We have mostly used the inversion procedure we have found to be the “assumed best procedure” for detection and characterisation of fracture zones in bedrock. This is not necessarily best procedure for detection and characterisation of soil layers, so we have also tried alternative procedures (Chapter 5.2.2 and 5.2.3).

The synthetic Dataset A has a **total soil thickness of 20 m** which is divided into two layers, a 5 m thick top layer with velocity 600 m/s (dry soil) and a second soil layer with velocity 1600 m/s (water saturated sand/gravel, fine graded fjord sediments). In Dataset A1 with one off-end shot 30 m away from the utmost receivers, the interpreted total soil thickness proved to be ca. 90 % of the true soil thickness both for the Hagedoorn interpretation (starting model) and the tomographic inversion. Increased number of off-end shots (30 + 60 m in Dataset A2 and 30 + 60 + 90 m in Dataset A3) improved the average total thickness calculations from 92.5 % to 95 %. However, the total soil thickness within the profile varied from ca. 16 to 20 m, giving a relatively high standard deviation (4.0 % to 7.5 %). The tomographic inversion using Hagedoorn’s interpretation as starting model, improved the total thickness interpretations slightly, especially for the A2 Dataset. Based on this, off-end shots at least 60 m from utmost receivers (three times the soil thickness) are recommended. Unfortunately, the tomographic inversion does not benefit much from this, since only off-end shots less than two receiver spacings (here 10 m) is used in the tomographic inversion (Intelligent Resources 2019b).

The synthetic Dataset B has a **total soil thickness of 40 m** which is divided into two layers, a 5 m thick top layer with velocity 600 m/s (dry soil) and a second soil layer with velocity 1600 m/s (water saturated sand/gravel, fine graded fjord sediments). In Datasets B1 and B2, which have the maximum length to off-end shots of 60 m, it was not possible to get response from the bedrock surface using the Hagedoorn method, and because of this, not at the tomographic inversion either. At Dataset B3, B4 and B5, having maximum length to the off-end shots equal 90, 120 and 150 m respectively, a quite good estimate of the total soil thickness was achieved. The average total soil thickness varied from 92.5 % to 96.7 % of the true total soil thickness. However, also in this case, the thickness varied from 34 m to 45 m along the profiles (85 % - 113 % of true depth), which is too much to get all calculations within +/- 10 % of the true soil thickness. The tomographic inversion showed a slightly better result ( $\approx 3$  %) than the Hagedoorn inversion for Dataset B3, almost the same for Dataset B4 and slightly less for Dataset B5. More off-end shots do not necessarily give better inversion results, and the Hagedoorn method may act as self-contained method for soil thickness calculations.

At Dataset C, having a **total soil thickness of 80 m**, only the Hagedoorn inversion of Dataset C4 (off-end shots at 60, 120, 180 and 240 m) were able to reach down to bedrock. Nine depth readings along the profile showed a total soil thickness from 67 to 72 m. In average the thickness was only 82.6 % of the true total soil thickness, which may be explained by few rays refracted from the bedrock surface. For Datasets A and B, we observed that more off-end shots improved the total soil thickness calculations. Most likely for Dataset C, off-end shots more than 240 m away from end receivers may improve the quality of total soil thickness calculations.

## Effect of hidden layer.

In Dataset F with **total soil thickness 40 m**, we introduced a **hidden layer (blind zone)** above bedrock. Dataset F1 had no hidden layer while F2, F3 and F4 had a hidden layer with velocity 2100 m/s and thickness 5, 10 and 20 m respectively. For the Hagedoorn method, it is physically impossible to see the hidden layer (Reynolds 2011). We wanted to see how big error we get with the Hagedoorn method, and whether the tomographic inversion could see the hidden layer or not.

In **Dataset F1**, without the hidden layer the interpreted soil thickness was 92.5 % of true soil thickness for the Hagedoorn interpretation and 93.8 % for the tomographic inversion and the standard deviation was low for both methods. For Dataset F2 (5 m thick hidden layer) these numbers were 89.2 % and 91.3 %. For Dataset F3 (10 m hidden layer) these numbers were 86.3 % and 89.1 % while the numbers for Dataset F4 (20 m hidden layer) was 82.2 % for both methods. As expected, the Hagedoorn method did not see the hidden layer, and the error in total soil thickness increased as the thickness of the hidden layer increased. Unfortunately, the tomographic inversion using the Hagedoorn inversion as starting model, do not see the hidden layer either. To see if we can overcome this problem, inversion using alternative starting model and alternative inversion software should be tested.

In **Dataset G** we introduced a 5 m thick top layer with velocity 600 m/s (dry soil) on top of a layer 2 with velocity 1600 m/s (water saturated sand/gravel or fine graded fjord sediments). The same hidden layer of velocity 2100 m/s as in Dataset F followed above bedrock. Layer number 1 (5 m thick) was indicated but with too low thickness (2.3 to 4.0 m, Table 6). However, we choose only one isoline ( $V = 750$  m/s) as interface indicator (dry soil on top of water saturated soil). Other choices would most likely give a better result.

Since the hidden layer (layer 3, 2100 m/s) was not seen in any of the datasets, the interpreted thickness of layer 2 showed values that varied in steps as the thickness of the hidden layer increased. With no hidden layer (Dataset G1) the interpreted thickness of layer 2 was 93 % of true thickness at the Hagedoorn method and 99.5 % for the tomographic inversion. For Dataset G4 (20 m hidden layer) these numbers increased almost 200 % of true layer 2 thickness. With a hidden layer in the geological section, it seems almost impossible to get a reliable result for individual layer thicknesses. Compared with Dataset F, the total soil thickness decreased by from 0 to 3% by introducing the top layer with velocity 600 m/s (Table 5 and Table 6). Introducing a low velocity top layer do not change the inversion very much, but the introduction of a hidden layer influences dramatically on the individual soil layer thicknesses.

Off-end shots are important for the Hagedoorn inversion of refraction seismic data, and since the Hagedoorn interpretation is used as a starting model, it is indirectly important for the tomographic inversion. The tomographic inversion does minor changes of the starting model. Inversion of Datasets A, B and C (total soil thickness 20, 40 and 80 m) showed inverted thicknesses that are less than the true total soil thickness.

NGU has experienced that the picking of midpoint breaks (Intelligent Resources 2019a), which are done semi-automatically, can be tuned in a way that can give very



good calculations of the total soil thickness (Rønning et al. 2020). This procedure was not explored when the present work was performed. Most likely, a better fit to true soil thicknesses could have been achieved by finetuning the inversion procedure by additional depth to bedrock information. It is not clear either if a manual crossover point pick instead of automatic pick of midpoint breaks, could give a better depth to bedrock interpretation. This should also have been explored.

### 5.2.2 Quality of depth to bedrock calculations using DeltatV method

The **DeltatV** starting model and the tomographic inversion using this as starting model, gives a gradual increase in velocity towards the depth (Figures 8 and 9). This means a velocity isoline must be selected as an indicator of depth to bedrock (total soil thickness). Unfortunately, the known bedrock surface did not follow one particular velocity isoline, but varied along the profiles. In our attempt to find the correct isoline, we identified the velocity isoline at eight or nine points along the profiles at end points and under each shot. For Dataset F1 the true bedrock isoline appeared at velocities from 2750 m/s to 3500 m/s (Table 7). When introducing a hidden layer (thickness 5 m, 10 m and 20 m in Datasets F2, F3 and F4) this interval increased stepwise and reached 3050 m/s to 4000 m/s for Dataset F4 (see Table 7). These undulations means that it is almost impossible to use one velocity isoline to describe depth to bedrock along the lines.

For **Dataset F1** (no hidden layer) the crossing of true depth to bedrock and velocity isoline appeared in average on 3083 m/s for the starting model and 3050 m/s for the tomographic inversion (Table 7). In this case the best indicator of bedrock surface is a velocity isoline about 3070 m/s. For Dataset F2 (5 m thick hidden layer) these numbers are 3200 m/s (starting model) and 3263 m/s for the tomographic inversion. In this case, a velocity isoline 3230 m/s could be an appropriate indicator for depth to bedrock. For Dataset F3 (10 m thick hidden layer) an appropriate indicator of depth to bedrock can be isoline 3340 m/s and for Dataset F4 (20 m thick hidden layer) this number is 3550 m/s. This means that the correct isoline for indicating bedrock surface, will also change according to the geological situation.

For **Dataset G**, with an extra top layer with velocity 600 m/s, an appropriate indicator of depth to bedrock was slightly less, 3020 m/s for Dataset G1, 3090 m/s for Dataset G2, 3210 m/s for Dataset G3 and 3520 m/s for Dataset G4. This means that not only the hidden layer, but also the top low velocity layer influences on which velocity isoline that can be used as depth to bedrock indicator. Since the physical model in a real situation is never known, one velocity isoline must be chosen as bedrock indicator, and this can be good for one geological model and not so good for another model. In our work we choose isoline 3250 m/s which is close to the average values both for Dataset F (Table 7) and Dataset G (Table 9).

Using velocity isoline 3250 m/s as indicator of depth to bedrock, the average depth to bedrock along the line for **Dataset F1** was ca. 42 m which is 105 % of the true depth (Table 8). However, the individual values along the profile varies from 38 m to 50 m (95 – 125 % of true depth) giving a standard deviation of average depth of 10 %. The interpreted depth to bedrock at the tomographic inversion, is 40.8 m (102 % of true depth) for Dataset F2, 39.5 m (99 %) for Dataset F3 and 37.9 m (95 %) for

Dataset F4. For **Dataset G**, with the low velocity top layer, the average deviation from true depth to bedrock increased by 3 to 5 % (Table 8 and Table 10) for the tomographic inversion. All average interpreted depths to bedrock values are within the traditional accuracy demand of +/- 10 % but the individual depths along the profiles vary from 78 % to 125 % of true depths.

To get a better fit in real studies additional information (eg. from drilling) is needed to tune the choice of velocity isoline, but the individual variations along the profile will most likely exist.

Despite the interpretation challenges, all DeltatV average depth to bedrock interpretations are within the traditional +/- 10 % accuracy uncertainties. However, individual values along the profiles could vary from 85 % to 125 % of true depth to bedrock for Dataset F and 83 % to 125 % for Dataset G.

### 5.2.3 Comparison of methods for depth to bedrock calculations

This study used six different inversion methods to calculate depth to bedrock: Hagedoorn starting model, Hagedoorn tomographic inversion, DeltatV starting model, DeltatV tomographic inversion all using Rayfract software. In addition, tomographic inversion using Geogiga software (two different inversion settings) and traditional manual Hagedoorn interpretation were used. As an indicator for depth to bedrock, we have used  $V=3250$  m/s isoline for all automatic methods. For the Hagedoorn method, this is not important since there is a sharp velocity gradient going from soil velocities ( $< 3000$  m/s) to bedrock velocities ( $> 3500$  m/s). For the tomographic inverted sections that use the DeltatV method (Rayfract software) and the Geogiga software, there is a smooth gradient variation in velocity with depth, and choosing the correct velocity isoline as bedrock indicator, is very important. We have chosen  $V=3250$  m/s, which seems to be a good average for the four different Dataset G models. Interpreted average depth to bedrock in meters at 8 or 9 points along the profiles are shown in Table 15. Table 16 shows interpreted depth to bedrock as a percentage of the true depth.

Table 15: Summary of interpreted average depth to bedrock in meters for Dataset G with total soil thickness 40 m, 5 m thick dry topsoil, 35 -15 m marine sediments ( $V= 1600$  m/s) and a hidden moraine layer ( $V= 2100$  m/s) with thickness 0 (G1), 5 m (G2), 10m (G3) and 20m (G4).

| Dataset (thicknesses (m)) | Hagedoorn Start-model | Hagedoorn Tomo-inv. | DeltatV Start-model | DeltatV Tomo-Inv | Geogiga Tomo-Inv. |
|---------------------------|-----------------------|---------------------|---------------------|------------------|-------------------|
| G1 (5 + 35 + 0)           | 36.6 ± 1.8            | 37.4 ± 2.2          | 42.1 ± 4.8          | 43.4 ± 4.7       | 41.6 ± 1.1        |
| G2 (5 + 30 + 5)           | 34.6 ± 2.0            | 35.6 ± 1.7          | 40.5 ± 5.0          | 42.1 ± 4.4       | 40.5 ± 1.5        |
| G3 (5 + 25 +10)           | 34.6 ± 1.5            | 34.8 ± 1.8          | 38.8 ± 6.0          | 40.9 ± 4.4       | 40.5 ± 1.6        |
| G4 (5 + 15 + 20)          | 32.3 ± 1.4            | 32.4 ± 1.2          | 37.6 ± 3.6          | 39.8 ± 4.9       | 37.8 ± 1.4        |
| All, average              | 34.5 ± 1.8            | 35.1 ± 2.1          | 39.8 ± 2.0          | 41.6 ± 1.6       | 40.1 ± 1.4        |

The traditional interpretation using Hagedoorn's method, performed by IMPAKT Geofysik, showed variation in depth to bedrock along the G1 Dataset from 37.3 m to 42.2 m which on average was 40.1 m ±1.5 m. Unfortunately, there was no time for interpreting datasets G2, G3 and G4.

Clearly, with the Hagedoorn method, the interpreted depth to bedrock is too low, both for the starting model and for the tomographic inversion using this. The depth to bedrock decreases while the thickness of the hidden layer increases. In these inversions, we have not used any known information to adjust the interpreted depth to bedrock. In the inversion of the real field data from the subsea tunnel project crossing the Romsdalsfjord, we saw that the process of choosing midpoint breaks for depth calculations could be fine-tuned to give reasonably good depth interpretations (Rønning et al. 2020). It is unclear if a time consuming manual pick of crossover points could improve the Hagedoorn depth to bedrock interpretations.

Table 16: Summary of interpreted average depth to bedrock in percent of true depth for Dataset G with total soil thickness 40 m, 5 m dry topsoil, 35 – 15 m marine sediments ( $V= 1600$  m/s) and a hidden marine layer ( $V= 2100$  m/s) with thickness 0 (G1), 5 m (G2), 10m (G3) and 20m (G4).

| Dataset (Thicknesses) | Hagedoorn Start-model | Hagedoorn Tomo-inv. | DeltatV Start-model | DeltatV Tomo-Inv | Geogiga Tomo-Inv. |
|-----------------------|-----------------------|---------------------|---------------------|------------------|-------------------|
| G1 (5 + 35 + 0)       | 91.4 ± 4.5            | 93.4 ± 5.5          | 105 ± 12            | 109 ± 12         | 104 ± 2.7         |
| G2 (5 + 30 + 5)       | 86.9 ± 5.0            | 89.1 ± 4.2          | 101 ± 13            | 105 ± 11         | 101 ± 3.9         |
| G3 (5 + 25 + 10)      | 86.4 ± 3.8            | 86.9 ± 4.4          | 97.0 ± 15           | 102 ± 11         | 101 ± 4.1         |
| G4 (5 + 15 + 20)      | 80.8 ± 3.5            | 80.9 ± 3.0          | 94.0 ± 9            | 100 ± 13         | 94.5 ± 3.5        |
| All                   | 86.4 ± 4.3            | 87.6 ± 5.2          | 99.3 ± 4.5          | 104 ± 3.9        | 100 ± 3.5         |

For the DeltatV method using Rayfract and for the Geogiga tomographic inversion, we must choose a velocity isoline that can be used as a bedrock indicator. We see from our analyses that the best-fitted isoline varies with the thickness of the hidden layer (Table 7, Table 9 and Table 11). In the analysis presented in Table 17, we used isoline  $V=3250$  m/s as bedrock indicator. This average fits well for Datasets G2 and G3 (5 and 10 m thick hidden layer) but not so well for dataset G1 and G4 (no and 20m thick hidden layer). Despite this, the interpreted average depths to bedrock are well within the traditional +/- 10 % accuracy uncertainties.

The **traditional interpretation** using Hagedoorn's method, performed by IMPAKT Geofysik, the average depth to bedrock along the G1 Dataset was 100 % ± 3.8 %.

The DeltatV interpretations using Rayfract software have a higher standard deviation in calculated average depth to bedrock (9 – 15 %) compared with the Hagedoorn method (3.0 – 5.5 %) and the Geogiga tomographic inversion (2.7 - 4.1 %). This difference is due to the local variations along the lines (unstable inverted models) and makes the DeltaV method less accurate along an interpreted line. The use of individual velocity isolines as bedrock indicator can increase the accuracy of the average depth to bedrock interpretations, but not the uncertainty along the lines.

It should be pointed out that in the DeltatV and the Geogiga inversions, the known information on depth to bedrock is used to select the best velocity isoline as bedrock indicator. In the tomographic inversions using Hagedoorn's method and the traditional interpretation, no a priori information is used. It seems that the traditional Hagedoorn interpretation shows up the best inversion. However, this is based on only one profile.

It should also be pointed out that the synthetic models used here have homogenous and smooth layers with a clear velocity contrasts. In this way, they are favourable for the Hagedoorn method. However, in the models we used real velocity values that are often seen in Norway.

### 5.3 Quality of soil material characterisation

Based on seismic velocities, a geologic interpretation of the refraction seismic data can be performed. Table 17 shows p-wave velocity in some geological materials observed through more than 50 years of refraction seismic work at NGU and by other companies in Norway. To some extent, it is possible to interpret soil materials. However, this is dependent on a good velocity calculation during the inversions.

Table 17: P-wave velocity in some soil and bedrock types (from [www.ngu.no](http://www.ngu.no)).

| Soil            | P-wave velocity (m/s) | Bedrock    | P-wave velocity (m/s) |
|-----------------|-----------------------|------------|-----------------------|
| Peat            | 150 – 500             | Sandstone  | 3000 – 3500           |
| Clay (dry)      | 600 – 1200            | Limestone  | 4000 – 6000           |
| Sand (dry)      | 400 – 900             | Dolomite   | 2500 – 6500           |
| Gravel (dry)    | 400 – 1000            | Quartzite  | 5500 – 6000           |
| Moraine (dry)   | 400 – 1600            | Granite    | 4800 – 5500           |
| Clay (wet)      | 1200 – 1600           | Gneiss     | 4700 – 5800           |
| Sand (wet)      | 1400 – 1800           | Diabase    | 5700 – 6500           |
| Gravel (wet)    | 1400 – 1900           | Gabbro     | 6200 – 6700           |
| Moraine (loose) | 1500 – 1900           | Ultramafic | 6500 – 7500           |
| Moraine (hard)  | 1900 – 2800           |            |                       |

#### 5.3.1 Detection and characterisation of soil layers using Hagedoorn's method

In Dataset A, the velocity of the first layer (600 m/s) was reconstructed quite well in the **Hagedoorn interpretation**. In the **tomographic inversion**, the velocity varied a bit, but always less than 1000 m/s. According to Table 14, this material should be interpreted as dry soil as assumed in the synthetic model. The velocity of the second layer (1600 m/s) was also well reconstructed in **Hagedoorn's** inversion, but the velocity varied from ca. 1500 m/s to ca. 2000 m/s in the **tomographic** inversion. A geological interpretation of this material should be water-saturated soil of different type. However, with velocities at almost 2000 m/s a misinterpretation of moraine material cannot be excluded.

In **Dataset B**, the velocity in the second soil layer varied from 1500 m/s to 2500 m/s for Datasets B1 and B2, where the length to the off-end shots was too short. In this case, materials that was supposed to be water-saturated clay-sand-gravel could be misinterpreted as hard moraine. Except for that, the soil velocities varied as in Dataset A, and it is possible to give a good geological interpretation. **Dataset C** (soil thickness 80 m) showed the same velocity distribution as in Dataset B and misinterpretation was possible where a too-short length to off-end shots prevented penetration to bedrock.

In **Datasets F and G**, where we introduced a third hidden soil layer (2100 m/s, moraine material) above bedrock, none of the interpretations were able to detect this layer. In this case, the moraine layer in the synthetic model has been disregarded.

In Dataset G with three soil layers, all tomographic inversion of all datasets indicate extensive **velocity inversions** (high velocity above a lower velocity) along the

sections in the tomographic inversion (Figure 9). Since the velocities in the synthetic model increase downwards, this is a false effect. For the other datasets, velocity inversion appears only locally in some discrete points. For the geological interpretation of real data, it suggests that an indication of a low-velocity zone under a high-velocity layer, might not be true.

In this work, we found the challenges of identifying the correct velocity in some layers, and that geologic misinterpretation of soil layers is possible. It was, therefore, interesting to see if alternative inversion methods can overcome the problem.

### 5.3.2 Detection and characterisation of soil layers using DeltatV method.

To get good inversions from the DeltatV method, short geophone spacings, short shot spacings and long profiles (> 500 m) are beneficial (Intelligent Resources 2019a). In our modelling, none of these assumptions are fulfilled. Despite this, we wanted to investigate the quality of inversions, especially for the Datasets F and G (two and three soil layers), where a hidden layer was introduced above bedrock.

Since the DeltatV inversion method results in a **gradual change in velocity** towards depth, a soil characterisation may be challenging. In Table 18, interpreted velocities that fell within the true layer interfaces are listed. For Dataset F1, the velocity in layer 1, which has a true velocity 1600 m/s, the values vary from ca. 1500 m/s to ca. 3500 m/s. When the hidden layer is introduced (Datasets F2, F3 and F4), the interval gets compressed but still, at Dataset F4, the velocity varies from 1500 to 2250 m/s. In the **Hagedoorn interpretation** (Figure 8, Table 5), the velocity in this layer was ca. 1600 m/s as in the synthetic model, and this method seems to be more suited for geological interpretations.

Table 18: DeltatV interpretation (starting model and tomographic inversion) of Dataset F (40 m soil cover). Inverted velocity variations within the true layer no.1 (1600 m/s) and layer no. 2 (2100 m/s).

| Dataset | Method                | Velocity interval.                        | Velocity interval.                        |
|---------|-----------------------|---|---|
|         |                       | Layer no. 1 (m/s).<br>True value 1600 m/s | Layer no. 2 (m/s).<br>True value 2100 m/s |
| F1      | Starting model        | 1500 - 3250                               | -   |
| F1      | Tomographic inversion | 1500 - 3500                               | -   |
| F2      | Starting model        | 1500 - 3000                               | 2500 - 3750                               |
| F2      | Tomographic inversion | 1500 - 3250                               | 2500 - 3750                               |
| F3      | Starting model        | 1500 - 3000                               | 2250 - 3750                               |
| F3      | Tomographic inversion | 1500 - 3000                               | 2200 - 3750                               |
| F4      | Starting model        | 1500 - 2250                               | 1800 - 4000                               |
| F4      | Tomographic inversion | 1500 - 2250                               | 1750 - 4000                               |

For the second soil layer, where the true velocity is 2100 m/s, the interpreted velocities greatly vary. In Dataset F2, the interpreted velocity varies from 2500 m/s to 3750 m/s, a velocity too high to represent the moraine layer in the synthetic model. In Dataset F3, the lower value in the interval (2200 and 2250 m/s) is close to the true value (2100 m/s), but most of the area fell within higher velocities that are too high to represent soil materials. In Dataset F4, the interval is even greater (1750 m/s to 4000 m/s). The first value could be interpreted as loose moraine, while the last can be

interpreted as bad rock quality. The gradual velocity variations make it difficult to make a geological interpretation of this layer. The Hagedoorn method (Chapter 4.5.1) was not able to detect this second hidden layer velocity either.

### 5.3.3 Comparison of methods for soil material characterisation

As for the **DeltatV** method using the Rayfract software, the **Geogiga** depth sections show up with a gradual increase in velocity. This makes it difficult to read out well-defined velocities in the soil, and soil characterisation is challenging.

The **traditional Hagedoorn** interpretation of Dataset G1 failed to detect the dry soil top layer with a velocity 600 m/s. The velocity of layer 2 (velocity 1600 m/s) was interpreted to 1520 - 1530 m/s, which is not far from the true value. Unfortunately, there was not time for interpreting the models with a hidden layer (G2, G3 and G4). Most likely, the manual interpretation would fail to detect the hidden layer.

Table 19: The ability to detect and characterise soil layers using Rayfract software (Hagedoorn and DeltatV including tomographic inversion using these as starting model), Geogiga tomographic inversion and traditional Hagedoorn manual interpretation.

| Method            | Velocity soil layer 1, V=600 (m/s) | Velocity soil layer 2, V=1600 (m/s) | Velocity soil layer 3, V=2100 (m/s) |
|-------------------|------------------------------------|-------------------------------------|-------------------------------------|
| Hagedoorn         | ≈ 600                              | 1500 - 2500                         | Not detected                        |
| Hagedoorn tomo    | ≈ 600                              | 1500 - 2500                         | Not detected                        |
| DeltatV           | Velocity gradient                  | Velocity gradient                   | Not detected                        |
| DeltatV tomo      | Velocity gradient                  | Velocity gradient                   | Not detected                        |
| Geogiga tomo      | Velocity gradient                  | Velocity gradient                   | Not detected                        |
| Traditional Hage. | Not detected                       | 1520 - 1530                         | Not tested                          |

The traditional and the automatic Hagedoorn inversion of this refraction seismic data seems to be better in the characterisation of soil material than the tomographic inversions using 1D gradient starting models for the tomographic inversions (DeltatV method using Rayfract and Geogiga tomographic inversion). The traditional interpretation failed to detect the 5 m thick dry soil layer on top. All methods failed to detect the third hidden layer (not tested with the Traditional interpretation).

## 5.4 General considerations

The DeltatV inversion of Dataset F, showed very good **RMS values** for the data fitting for the starting model (≈ 4.7 % or ≈ 1.3 m/s) and extremely good for the tomographic inverted models (0.1 – 0.2 % or ≤ 0.04 m/s, Figure 10). For the Hagedoorn starting model (Figure 8) these numbers were slightly lower (< 2.0 % or ≈ 0.5 m/s) but the tomographic inversion using Hagedoorn inversion as starting model showed slightly higher values than the DeltatV tomographic inversion (0.3 – 0.5 %, 0.07 – 0.12 m/s, Figure 8). Visually, the Hagedoorn interpretation, both the starting model and the tomographic inverted models, gives a better image of the synthetic model. In this case, where we have well defined homogeneous soil layers, the Hagedoorn method

is well suited for inversion of the refraction seismic data. In other cases, where there is a gradual change in velocity towards the depth, the DeltatV method can most likely give better results. A very good RMS error is no guarantee for a good velocity section. A priori knowledge of what geological model we are working on is necessary to choose the best inversion procedure for the soil mapping and characterisation.

One limitation with the tomographic inversion using Rayfract, is the possibility to use information from off-end shots. Since single spreads have no receivers where off-end shots are located, the velocity distribution will be unknown outside the receiver spread, making it impossible to achieve reliable velocity sections. In such cases, it is recommended to have several spreads with overlapping receivers (Intelligent Resources 2019b).

In this work, we have seen tomographic inverted velocity sections that indicate velocity inversion (a low velocity underneath a higher velocity). Since we know the synthetic model and no velocity inversions exists, this must be a false effect. Indicated velocity inversions in the tomographic inverted sections are not necessarily true.

The Rayfract software includes a lot of inversion procedures and what we have tested, is necessarily not the best. After this modelling work was finished, a new version of the software was published. (v. 4.01). This version contains a new Wavelength-Dependent Velocity Smoothing (WDVS, Zelt & Chen 2016) that gives a better WET resolution and sharper imaging of layer boundaries if tuned correctly. This routine, along with others, should be tested to see if a more compressed velocity section can be achieved, especially with the DeltatV method.

To fully understand how the automatic inversion of refraction seismic data, that uses both the Rayfract software and other software, can be used to locate and characterise fracture zones in bedrock, calculate depth to bedrock and characterise soil material, even more modelling is needed.

## 6. CONCLUSIONS

NGU has chosen to use the Rayfract software for inversion of refraction seismic data. To test an alternative inversion software from Geogiga, we got help from Roger Wisén at IMPAKT Geofysik. In the present work we have concentrated on modelling of fracture zone mapping and characterisation as well as soil mapping and characterisation. From the present work we can conclude as follows:

### **Detection and characterisation of fracture zones:**

- The automatic Hagedoorn inversion of refraction seismic data gives a good image of fracture zones in bedrock under limited (< 20 m) soil cover. A thicker soil cover presents challenges and demands traditional interpretation.
- Due to poor resolution, thick fracture zones under a thick soil cover (> ca. 20 m) may consist of several thinner fractured zones.
- Tomographic inversion using Hagedoorn's inversion as starting model can improve the velocity sections and sometimes process away artificial effects from the Hagedoorn inversion.
- Increased number of off-end shots improves both the Hagedoorn and the tomographic inversion slightly.

- The DeltatV method is not as well suited for fracture zone mapping and characterisation as Hagedoorn's method.
- The Gogigiga software did not indicate fracture zones in bedrock the way the inversion was performed in this work.
- Traditional interpretation of refraction seismic seems to be the best method for detection and characterisation of fracture zones under a thicker soil cover.

#### **Detection and characterisation of soil layers:**

- The automatic Hagedoorn inversion of refraction seismic data gives a good image of the soil layers as long as the assumptions for using the method are fulfilled (increased velocity with depth, sub-horizontal homogenous layers, large velocity contrast).
- Tomographic inversion using the Hagedoorn inversion as starting model can improve the total soil thickness calculations.
- At shallow depths, an accuracy of 90 to 95 % of the average true soil thickness can be achieved with the Hagedoorn's method and following tomographic inversion without any a priori information.
- Hidden layers of increasing thickness may reduce the accuracy to ca. 80 % of true soil thickness. However, individual variations along the profiles may be larger.
- Except in the case of hidden layers, the Hagedoorn inversion may give good velocity estimations that can be used for soil material characterisation.
- The DeltatV inversion method shows a gradual increase of the velocity with depth, and a velocity isoline must be chosen as an indicator for bedrock surface. In the present work, we were able to find a velocity isoline that gave an average total thickness within +/- 8 % of the true soil thickness for the hidden layer models, which is very good. However, variations along the profiles varied from 78 % to 125 % of the real soil thickness. The challenge is to select the right velocity isoline since it will change for different geological models.
- The gradient velocity distribution in the DeltatV inversion makes soil material characterisation challenging.
- The Geogiga inversion gave the best depth to bedrock interpretation, but the soil characterisation was challenging.
- The DeltatV and the Geogiga inversions used known depth to bedrock information when selecting velocity isoline as bedrock indicator.
- Traditional interpretation of one profile showed a very good depth to bedrock values, but failed to see more than one soil layer.

#### **General considerations:**

- At least, one off-end shot should be more than three times the soil thickness away from both ends of the receiver spread.
- A low RMS error do not guarantee for a correct velocity section.
- Velocity inversion in the tomographic inverted data can be a false effect.
- Tomographic inversion using Rayfract do not account for off-end shots, which is a limitation.
- Used in the right way and with limited soil thickness, the Rayfract software can be used for the location and characterisation of fractured zones in bedrock as well as mapping and characterisation of soil layers. However, hidden layers (blind zones) seem to be a problem.



- In this study we have tested just a few models, and during the work the Rayfract software is upgraded with new routines. More modelling is needed to get better understanding of how automatic inversion of refraction seismic data works, also with other available software.

## 7. REFERENCES

- Ali Ak, M. 1990: An analytical raypath approach to the refraction wavefront method. *Geophysical Prospecting*, vol. 38, pp. 971 – 982.
- Bruckl, E. 1987: The Interpretation of Traveltime Fields in Refraction Seismology. *Geophysical Prospecting*, vol. 35, pp. 973 – 992.
- Gebrande, H. & Miller, H. 1985: Refraktionsseismik (in German). In: F. Bender (Editor), *Angewandte Geowissenschaften II*. Ferdinand Enke, Stuttgart; pp. 226-260. ISBN 3-432-91021- 5.
- Geogiga 2019: Geogiga DW Tomo 9.1 — Refraction Tomography Software  
<https://www.geogiga.com/en/dwtomo.php>
- Golden Software, 2018: Surfer 15, ver. 15.4.354 - Powerful Contouring, Gridding & 3D Surface Mapping Software. Golden Software, LLC, Colorado, USA.
- Hagedoorn, J.G. 1959: The Plus-Minus method of interpreting seismic refraction sections. *Geophysical Prospecting* 7 (2), pp.158 – 182.
- Intelligent Resources 2019a: Rayfract Seismic Refraction & Borehole Tomography-Subsurface Seismic Velocity Models for Geotechnical Engineering and Exploration. Downloaded from <http://rayfract.com>
- Intelligent Resources 2019b: Rayfract help. Download from <http://rayfract.com>
- Reynolds, J. M. 2011: An Introduction to Applied and Environmental Geophysics. Wiley & Sons, West Sussex, UK (2<sup>nd</sup> edition).
- Rønning, J.S., Tassis, G., Kirkeby, T. & Wåle, M. 2016: Retolkning av geofysiske data og sammenligning med resultater fra tunneldriving, Knappetunnelen ved Ringveg Vest i Bergen. NGU Rapport 2016.048 (48s.).  
[http://www.ngu.no/upload/Publikasjoner/Rapporter/2016/2016\\_048.pdf](http://www.ngu.no/upload/Publikasjoner/Rapporter/2016/2016_048.pdf)
- Rønning, J.S., Tassis, G., Kirkeby, T. & Wåle, M. 2019a: Reprosessering og ny samtolking av geofysiske data med resultater fra tunneldriving, Knappetunnelen ved Ringveg Vest i Bergen. NGU Rapport 2019.014 (57s.).  
[https://www.ngu.no/upload/Publikasjoner/Rapporter/2019/2019\\_014.pdf](https://www.ngu.no/upload/Publikasjoner/Rapporter/2019/2019_014.pdf)
- Rønning, J.S., Tassis, G., Kirkeby, T., Wåle, M. & Rohdewald, S. 2019b: Hvordan bør refraksjonsseismikken utføres, tolkes og presenteres? Tradisjonell tolking eller tomografisk inversjon. Bergmekanikkdagen, Oslo, 21. nov. 2019. Artikkel 21.

- Rønning, J.S., Tassis, G., Kavli, A., Wisén, R. & Åndahl, T. 2020: Kvalitet på tolking av seismikk. Eksempler fra E39 Kryssing av Romsdalsfjorden. NGU Rapport 2020.040.
- Sjøgren, B. 1984: Shallow Refraction Seismics. Chapman & Hall, London/New York.
- Tassis, G., Rønning, J.S. & Rohdewald, S. 2017: Refraction seismic modelling and inversion for the detection of fracture zones in bedrock with the use of Rayfract® software. NGU Report 2017.025 (62pp.).  
[https://www.ngu.no/upload/Publikasjoner/Rapporter/2017/2017\\_025.pdf](https://www.ngu.no/upload/Publikasjoner/Rapporter/2017/2017_025.pdf)
- Tassis, G., Rodewald, S. & Rønning J.S. 2018: Tomographic Inversion of Synthetic Data Using Various Starting Models in Rayfract® software. NGU Report 2018.015 (45pp.). [https://www.ngu.no/upload/Publikasjoner/Rapporter/2018/2018\\_015.pdf](https://www.ngu.no/upload/Publikasjoner/Rapporter/2018/2018_015.pdf)
- Westerdahl, H. 2003: Seismisk modellering. Modellering av seismiske data over løsmassefylte depresjoner, svakhetssoner og ved kabelheng. Miljø- og samfunnstjenlige tunneler, Rapport 32. Statens vegvesen.  
[https://vegvesen.brage.unit.no/vegvesen-xmlui/bitstream/handle/11250/190422/intern\\_rapport\\_2328.pdf?sequence=1&isAllowed=y](https://vegvesen.brage.unit.no/vegvesen-xmlui/bitstream/handle/11250/190422/intern_rapport_2328.pdf?sequence=1&isAllowed=y)
- Wåle, M. 2009: Refraksjonsseismiske undersøkelser Ringveg vest, byggetrinn 2 Sandeide-Liavatnet. GeoPhysix, Rapport nr. 09171 (in Norwegian).
- Zelt, C.A. & Chen, J. 2016: Frequency-dependent travelttime tomography for near-surface seismic refraction data. Geophys. J. Int. (2016) 207, 72 – 88. doi:10.1093/gji/ggww269.



GEOLOGICAL  
SURVEY OF  
NORWAY

· NGU ·

Geological Survey of Norway  
PO Box 6315, Sluppen  
N-7491 Trondheim, Norway

Visitor address  
Leiv Eirikssons vei 39  
7040 Trondheim

Tel (+ 47) 73 90 40 00  
E-mail [ngu@ngu.no](mailto:ngu@ngu.no)  
Web [www.ngu.no/en-gb/](http://www.ngu.no/en-gb/)